DOI: 10.1002/ejoc.200700505

meso,meso-Linked and Triply Fused Diporphyrins with Mixed-Metal Ions: Synthesis and Electrochemical Investigations

Leslie-Anne Fendt,[a] Hongjuan Fang,[a] Marta E. Plonska-Brzezinska,[b,c] Sheng Zhang,[b] Fuyong Cheng,[a] Christophe Braun,[a] Luis Echegoyen,*[b] and François Diederich*[a]

Dedicated to Professor Dr. Gerard van Koten on the occasion of his 65th birthday

Keywords: Diporphyrins / Electrochemistry / UV/Vis spectroscopy / Electrostatic interactions / Conjugation

A novel series of biaryl-type, *meso*,*meso*-linked and planar, triply fused diporphyrin derivatives was prepared and fully characterized together with the corresponding monoporphyrin control compounds. They feature peripheral *meso*-3-cyanophenyl and *meso*-3,5-cyanophenyl groups, which have previously been shown to undergo transformation into malonates without perturbation of the porphyrin core and subsequent Bingel addition to fullerene C_{60}. The tetrapyrrolic metal binding sites in the diporphyrin arrays are either complexed to two Zn^{II} or Cu^{II} ions, or, in a mixed coordination, to one Cu^{II} and one Zn^{II} ion; alternatively, one or both sites remain unoccupied. The interaction between the differentially metallated porphyrin rings was systematically investigated by UV/Vis spectroscopy and electrochemistry. Cyclic voltammetry and differential pulse voltammetry reveal that electronic communication in the diporphyrin arrays varies strongly with the mode of connection (*meso*,*meso*-linked or triply fused), the nature of the bound metal ion, and the number of peripheral cyano groups. The electrochemical HOMO–LUMO gap in both series of diporphyrins is strongly but differentially affected by the choice of the inserted metal ions.

Introduction

In recent years, Osuka and coworkers introduced several families of oligoporphyrin arrays in which individual porphyrin rings are linked together either by single bonds in a biaryl-type fashion (*meso*,*meso*-linked) or by triple fusion with formation of planar, sheet-like structures.[1] They are among the most promising new scaffolds for advanced materials applications,[2] and consequently, their optical and photophysical properties are increasingly being investigated.[3,4] We have conjugated singly *meso*,*meso*-linked and triply fused oligoporphyrins with C_{60} and studied in detail the electrochemical properties of the resulting dyads, thereby demonstrating their exceptional multicharge storage capacity.[5] In the course of that work, we became interested in investigating the properties of mixed-metal diporphyrins[6] and, ultimately, the interactions of the differentially metallated porphyrins with fullerenes both in solution[7] and on surfaces.[8] Here, we describe the synthesis and study of a series of mixed-metal diporphyrins[9–13] that bear *meso*-3-cyanophenyl and *meso*-3,5-dicyanophenyl rings in their periphery for further transformation into malonates and subsequent conjugation to fullerenes by Bingel addition.[5] We analyze the electronic communication between differentially metallated porphyrin ring centers in the arrays and show its strong dependence on the nature of the linkage. Electrochemistry is the method of choice for such investigation; despite the fact that a very large number of covalent and supramolecular oligoporphyrin assemblies have been prepared as models for photosynthetic reaction centers, light-harvesting antenna complexes, or photonic devices, only a limited number of electrochemical studies on oligoporphyrin arrays have been described.[4,5b–5d,14–17] Figure 1 shows all diporphyrins (**6**–**21**) and monomeric controls (**1**–**5**) included in this investigation.

[a] Laboratorium für Organische Chemie, ETH-Hönggerberg, HCI,
8093 Zürich, Switzerland
Fax: +41-44-632-1109
E-mail: diederich@org.chem.ethz.ch
[b] Department of Chemistry, Clemson University,
Clemson, SC 29634, USA
Fax: +1-864-656-6613
E-mail: luis@clemson.edu
[c] Institute of Chemistry, University of Bialystok,
15-399 Bialystok, Poland
Supporting information for this article is available on the WWW under http://www.eurjoc.org or from the author.

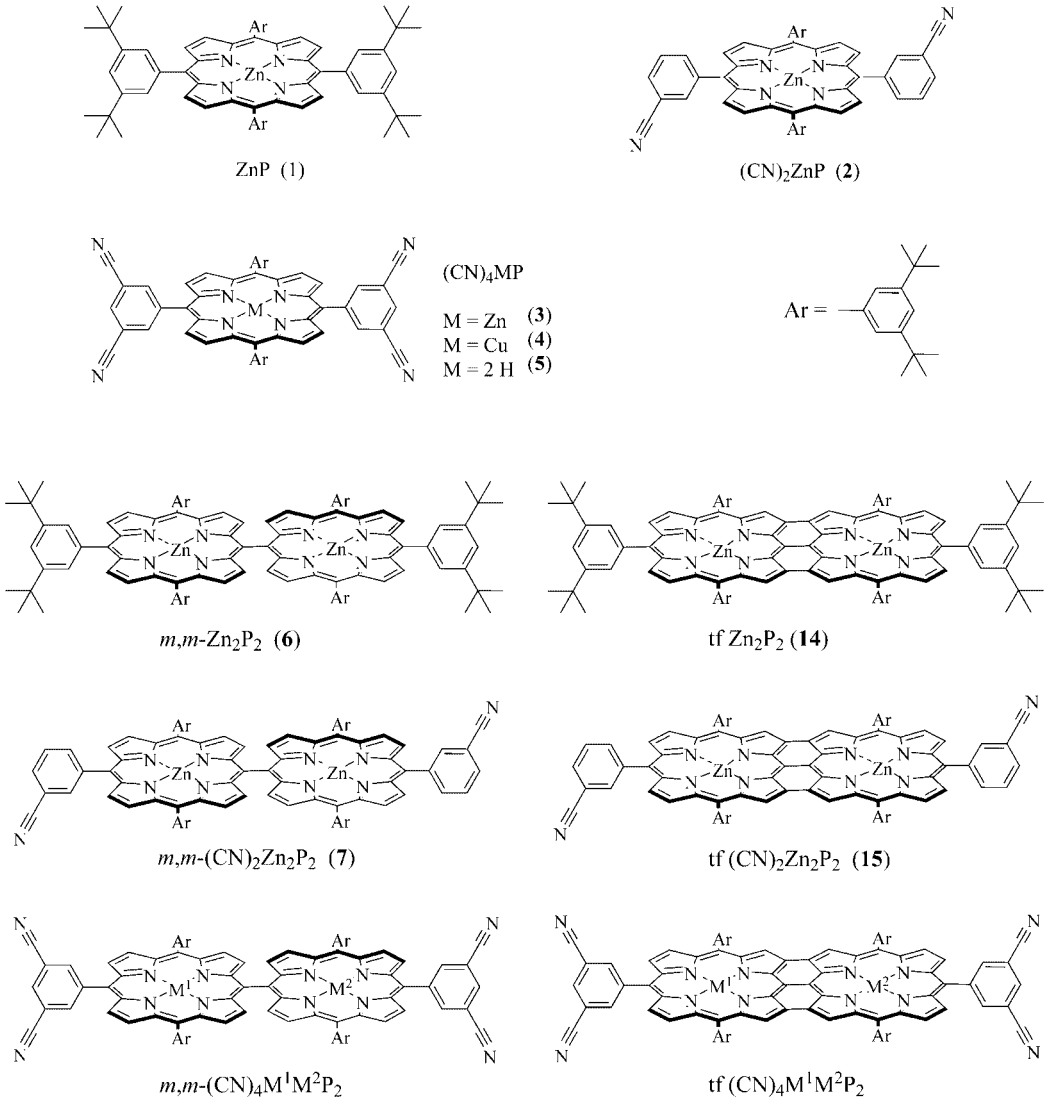

$M^1 = M^2 = Zn$	(**8**)	$M^1 = M^2 = Zn$	(**16**)
$M^1 = M^2 = Cu$	(**9**)	$M^1 = M^2 = Cu$	(**17**)
$M^1 = Zn, M^2 = 2\ H$	(**10**)	$M^1 = Zn, M^2 = 2\ H$	(**18**)
$M^1 = Cu, M^2 = 2\ H$	(**11**)	$M^1 = Cu, M^2 = 2\ H$	(**19**)
$M^1 = Zn, M^2 = Cu$	(**12**)	$M^1 = Zn, M^2 = Cu$	(**20**)
$M^1 = M^2 = 2\ H$	(**13**)	$M^1 = M^2 = 2\ H$	(**21**)

Figure 1. Overview of *meso,meso*- (*m,m*-) singly linked and triply fused (tf) diporphyrins and monomeric controls included in this investigation.

Porphyrins are abbreviated as P_n, where *n* represents the number of incorporated porphyrin units.

Results and Discussion

Synthesis of Monoporphyrin Derivatives

Tetracyano-substituted Zn^{II} porphyrin $(CN)_4ZnP$ (**3**) was synthesized in a Suzuki cross-coupling between diiodoporphyrin **22**[5b,5d] and boronate **23**, obtained from 5-bromophthalonitrile[18] and bis(pinacolato) diboron (Scheme 1). Demetallation with TFA provided the free-base porphyrin $(CN)_4H_2P$ (**5**), which was remetallated with $Cu(OAc)_2$ in $MeOH/CHCl_3$ to give $(CN)_4CuP$ (**4**).

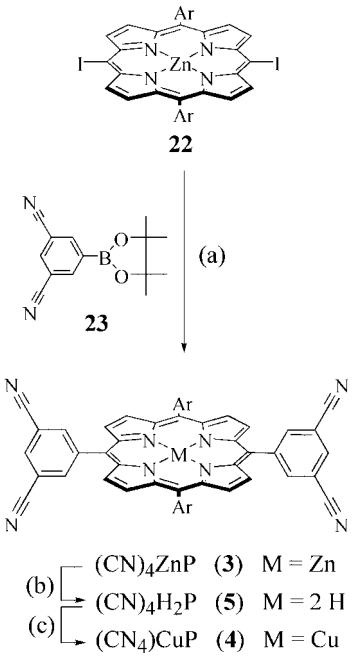

Scheme 1. Synthesis of monoporphyrins: (a) **23**; Cs_2CO_3; [$Pd(PPh_3)$]; PhMe; 140 °C; 20 h; 70%; (b) TFA; $CHCl_3$; 20 °C; 2 h; quant.; (c) $Cu(OAc)_2$; MeOH/$CHCl_3$, 1:1; Δ; 2 h; 92%. TFA = trifluoroacetic acid, Ar = 3,5-bis(*tert*-butyl)phenyl.

Synthesis of *meso*,*meso*-Linked Diporphyrin Derivatives

Ag^I-promoted oxidative coupling[1a,19] of dicyanoporphyrin **24**, obtained by cross-coupling between the corresponding iodoporphyrin[5d] and **23**, afforded the bis(zinc) derivative *m*,*m*-$(CN)_4Zn_2P_2$ (**8**) (Scheme 2). Demetallation provided *m*,*m*-$(CN)_4H_4P_2$ (**13**) and subsequent remetallation gave *m*,*m*-$(CN)_4Cu_2P_2$ (**9**). The latter compound cannot be prepared by oxidative dimerization of the corresponding Cu^{II} monoporphyrin; rather, such coupling leads to single-bond connection between the β positions, which was explained by molecular orbital considerations.[15c]

The synthesis of hybrid *meso*,*meso*-diporphyrins with two different metal ions or with one free-base tetrapyrrolic site was best accomplished by forming the bridging C–C single bond by Suzuki cross-coupling.[19] For this purpose, Zn^{II} monoporphyrin **24** was iodinated (I_2, $AgPF_6$) to give iodoporphyrin **25**. Demetallation afforded **26**, whereas coupling of **25** with pinacolborane yielded **27**. Suzuki cross-coupling of iodide **26** with boronate ester **27** subsequently provided *m*,*m*-$(CN)_4ZnH_2P_2$ (**10**), which was metallated with $Cu(OAc)_2$ to yield *m*,*m*-$(CN)_4ZnCuP_2$ (**12**). Demetallation of boronate **27** gave **28**, which was remetallated with Cu^{II} to provide monoporphyrin **29**, and cross-coupling between **26** and **29** afforded *m*,*m*-$(CN)_4CuH_2P_2$ (**11**). Alternatively, **11** was also obtained by cross-coupling of iodide **30**, obtained by insertion of Cu^{II} into **26**, and free-base boronate **28** (Scheme 3).

Synthesis of Triply Fused Diporphyrin Derivatives

The oxidative conditions [$Sc(OTf)_3$, DDQ] introduced by Osuka and coworkers were applied to the formation of triply fused diporphyrins starting from monoporphyrins (Scheme 4).[2a,20] Thus, coupling of monoporphyrin **24** afforded tf $(CN)_4Zn_2P_2$ (**16**). Alternatively, the latter was also prepared by oxidation of *meso*,*meso*-diporphyrin **8** with DDQ. Oxidation of *m*,*m*-$(CN)_4ZnH_2P_2$ (**10**) with DDQ afforded the tf $(CN)_4ZnH_2P_2$ hybrid system **18**, and metallation with $Cu(OAc)_2$ provided mixed-metallated tf $(CN)_4ZnCuP_2$ (**20**).

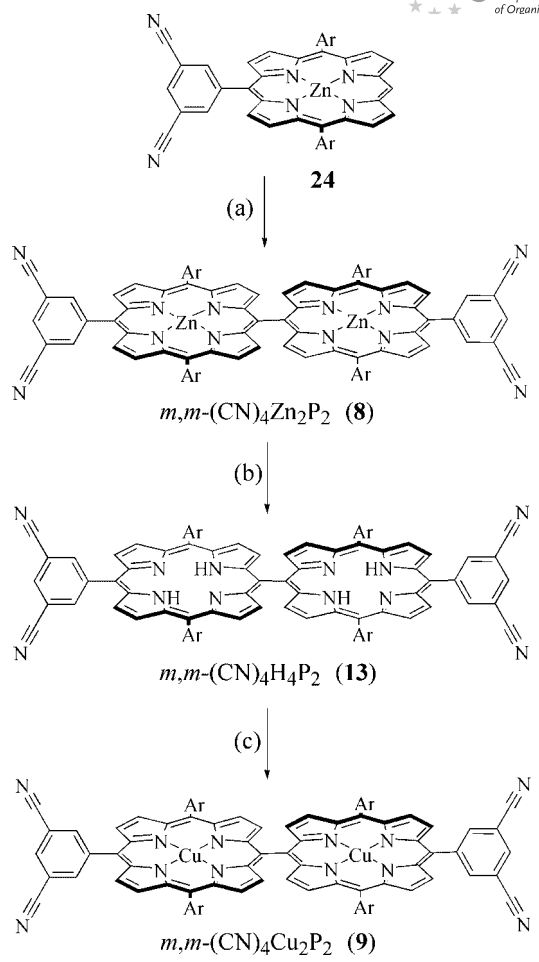

Scheme 2. Synthesis of symmetric *meso*,*meso*-linked diporphyrins: (a) $AgPF_6$; $CHCl_3$; Δ; 18 h; 85%; (b) conc. HCl/MeOH, 1:1; 10 min; 20 °C; quant.; (c) $Cu(OAc)_2$; MeOH/$CHCl_3$, 1:1; Δ; 20 h; quant. Ar = 3,5-bis(*tert*-butyl)phenyl.

Again for electronic reasons, tf $(CN)_4Cu_2P_2$ (**17**), tf $(CN)_4CuH_2P_2$ (**19**), and tf $(CN)_4H_4P_2$ (**21**) could not be prepared by the route described above. Demetallation of tf $(CN)_4Zn_2P_2$ (**16**) afforded **21**, which was remetallated with $Cu(OAc)_2$ to afford a mixture of tf $(CN)_4Cu_2P_2$ (**17**) and tf $(CN)_4CuH_2P_2$ (**19**). The mixture of **17** and **19** was inseparable by chromatography methods; thus, separation was eventually achieved by metallation of the mixture with MgI_2 to transform **19** into tf $(CN)_4CuMgP_2$ (**31**). Gratifyingly, **17** and **31** now featured sufficiently different polarity to allow chromatographic separation. Finally, demetallation with TFA afforded tf $(CN)_4CuH_2P_2$ (**19**).[21]

As control compounds for the electrochemical studies, other sets of monoporphyrins [ZnP (**1**),[22] $(CN)_2ZnP$

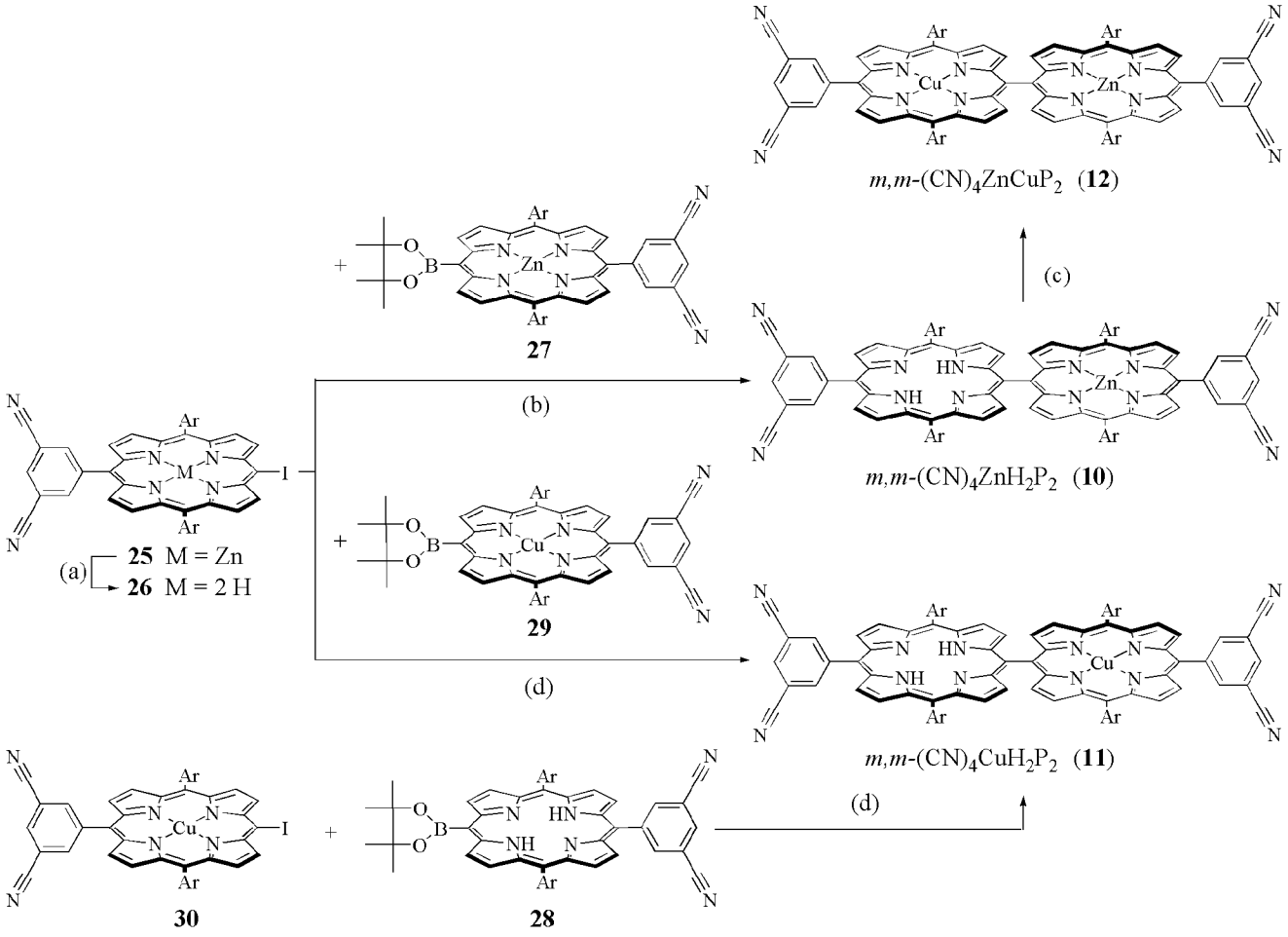

Scheme 3. Synthesis of hybrid *meso*,*meso*-linked diporphyrins: (a) TFA; CH_2Cl_2; 20 °C; 2 h; 90%; (b) Cs_2CO_3; [$Pd(PPh_3)_4$]; PhMe; 80 °C; 3 h; 45%; (c) $Cu(OAc)_2$; MeOH/$CHCl_3$, 1:1; Δ; 2 h; 92%; (d) Cs_2CO_3; [$Pd(PPh_3)_4$]; PhMe/DMF, 2:1; 80 °C; 3 h; 75% (from **29**); 99% (from **28**). Ar = 3,5-bis(*tert*-butyl)phenyl; DMF = dimethylformamide.

(**2**)[8a,23]], *meso*,*meso*-linked diporphyrins [*m*,*m*-Zn_2P_2 (**6**),[24] *m*,*m*-$(CN)_2Zn_2P_2$ (**7**)[5b,5d]], and triply fused diporphyrins tf Zn_2P_2 (**14**),[25] tf $(CN)_2Zn_2P_2$ (**15**),[5b,5d] were prepared following literature protocols.

^{1}H NMR Spectroscopy

All new mono- and diporphyrins were fully characterized as colored, high-melting stable solids. In the high-resolution matrix-assisted laser-desorption-ionization mass spectra (HR-MALDI-MS), the molecular ions appear as base peaks with little or no fragmentation seen. Representative ^{1}H NMR spectroscopic data ($CDCl_3$) for a selected series of compounds are depicted in Figure 2.

The β-protons of monoporphyrins **3** and **5** and the "outer" β-protons of the *meso*,*meso*-linked diporphyrins (H^b, H^c, and H^d in **8**, **10**, and **13**) appear at similar chemical shifts between 8.56 and 9.13 ppm. In contrast, the "inner" β-protons H^a of the *meso*,*meso* derivatives are shifted upfield into the range of 7.98 to 8.15 ppm, which is readily explained by the shielding from the neighboring orthogonal porphyrin moiety. In contrast, the resonances of both "inner" and "outer" β-protons in the triply fused diporphyrins are shifted upfield. Simultaneously there is a dramatic downfield shift of the inner NH resonances in triply fused free-base derivative **21** (δ = 1.34 ppm) relative to the corresponding resonance in *meso*,*meso* derivative **13** (δ = –2.27 ppm) and monoporphyrin **5** (δ = –2.67 ppm). We take this as an indication that aromaticity, as measured by ring-current effects, is reduced in triply fused porphyrins relative to that in monoporphyrins. On the other hand, the explanation might not be that straightforward because the inner NH resonances in both the *meso*,*meso*- and triply fused monozinc(II) derivatives appear at similar chemical shift [–2.14 (for **10**) and –2.18 ppm (for **18**)]. Overall, the observed trends in chemical shift changes agree well with those reported by Osuka and coworkers.[15c]

UV/Vis Spectroscopy

The electronic absorption spectroscopic data in $CHCl_3$ at 293 K are summarized in Table 1. Spectral comparisons between differentially metallated mono- and diporphyrins are shown in Figure 3.

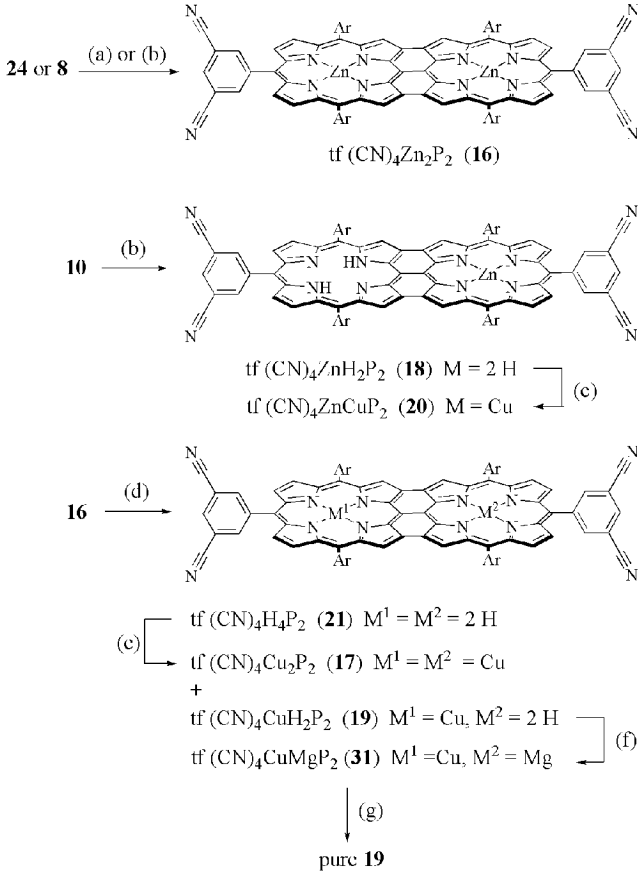

Scheme 4. Synthesis of triply fused diporphyrins: (a) $Sc(OTf)_3$; DDQ; PhMe; Δ; 3 h; 85%; (b) $Sc(OTf)_3$; DDQ; PhMe; Δ; 1 h; 90% (**16**); 20% (**18**); (c) $Cu(OAc)_2$; MeOH/$CHCl_3$, 1:1; Δ; 2 h; quant.; (d) conc. HCl/MeOH, 1:1; 10 min; 20 °C; quant.; (e) $Cu(OAc)_2$; MeOH/$CHCl_3$, 1:1; 20 °C; 2 h; inseparable mixture of **17** and **19**; (f) MgI_2; DIEA; CH_2Cl_2; 30 min; 20 °C; 78% (pure **17**); 17% (pure **31**) (over 2 steps); (g) TFA; $CHCl_3$; 14 h; 20 °C; quant. Tf = CF_3SO_2, DDQ = 2,3-dichloro-5,6-dicyano-*p*-benzoquinone, DIEA = diisopropylethylamine, Ar = 3,5-bis(*tert*-butyl)phenyl.

In the series of monoporphyrins, the maximum of the Soret band shifts slightly to higher energy upon moving from the Zn^{II}, to the free-base, and to the Cu^{II} derivative (Figure 3, top). The *Q*-bands show the expected characteristic splitting with two maxima for the Zn^{II}, four maxima for the free-base, and two weaker maxima for the Cu^{II} derivative.[26,27] With increasing number of peripheral CN groups, the Soret band shifts bathochromically (**1**→**2**→**3**, Table 1).

The Soret bands of the *meso,meso*-linked diporphyrins are split and broadened due to exciton chirality coupling (Figure 3, middle).[5c,5d,12c,28] The *Q*-bands display the features expected from the spectra of the monoporphyrins, with *m*,*m*-$(CN)_4ZnH_2P_2$ (**10**) notably showing the four maxima at similar wavelengths to those recorded for the free-base monoporphyrin. While the higher-energy Soret band (Table 1) displays a bathochromic shift upon introduction of 2 and 4 peripheral CN groups, respectively, thereby reminding the spectral features seen in the corresponding series of monoporphyrins, this is not the case for the second, lower-energy Soret band.

The higher-energy Soret band of the triply fused diporphyrins appears at wavelengths similar to those measured for the *meso,meso*-linked derivatives. In contrast, the lower-energy Soret band encounters a larger bathochromic shift (Figure 3, bottom; Table 1). No characteristic changes in absorption as a result of the introduction of peripheral CN groups are observed. The most prominent feature in the spectra of the triply fused diporphyrins is the very large bathochromic shift of the three to four observed *Q*-bands, with the end absorption appearing in the near infrared around 1200 nm.[1e,2a,3e] This shift is a direct result of the greatly extended π-electron delocalization in the triply fused diporphyrins relative to that in monoporphyrins and *meso,meso*-linked diporphyrins.

Electrochemistry

Significant information about the interaction between two different metal-ion sites in *meso,meso*- and triply fused diporphyrins was provided in a comprehensive electrochemical investigation. The redox properties of the mono- and diporphyrins were analyzed by cyclic voltammetry (CV) and differential pulse voltammetry (DPV) in CH_2Cl_2 (+0.1 M nBu_4NPF_6). All potentials are reported relative to the ferrocene/ferricinium (Fc/Fc^+) couple used as internal reference. The data are summarized in Table 2.

Monoporphyrins generally exhibit similar electrochemical properties, capable of being stepwise oxidized or reduced by two electrons to give π-cation radicals and dications or π-anion radicals and dianions, respectively.[29a] Early electrochemical studies demonstrated that most of the porphyrins exhibited a reasonably constant potential difference between the first and the second macrocycle-centered oxidations or between the first and second macrocycle-centered reductions, as well as a similar HOMO–LUMO gap of 2.25 ± 0.15 V.[26b] The HOMO–LUMO energy level diagram constructed from the electrochemical data revealed destabilization of the HOMO level and stabilization of the LUMO level upon dimer formation.[30]

When porphyrins with nonelectroactive centers (Zn, Cu) are investigated, the redox processes involve the π-system only.[15c] When the two rings are sufficiently apart and not conjugated, the dimer nearly behaves as two independent monomers. A two-electron oxidation process formally gives rise to a π-cation diradical. When the two rings are very close and/or conjugated, strong π–π interactions generate mixed valence behavior. In this situation, the first oxidation process splits into two one-electron steps.[31,15c]

The results demonstrate that the two series of dimers (*meso,meso*-linked and triply fused) give rise to a complex redox situation. All of the different possible redox pathways for the diporphyrins are shown in Scheme 5, which was previously proposed by Collman and coworkers.[31]

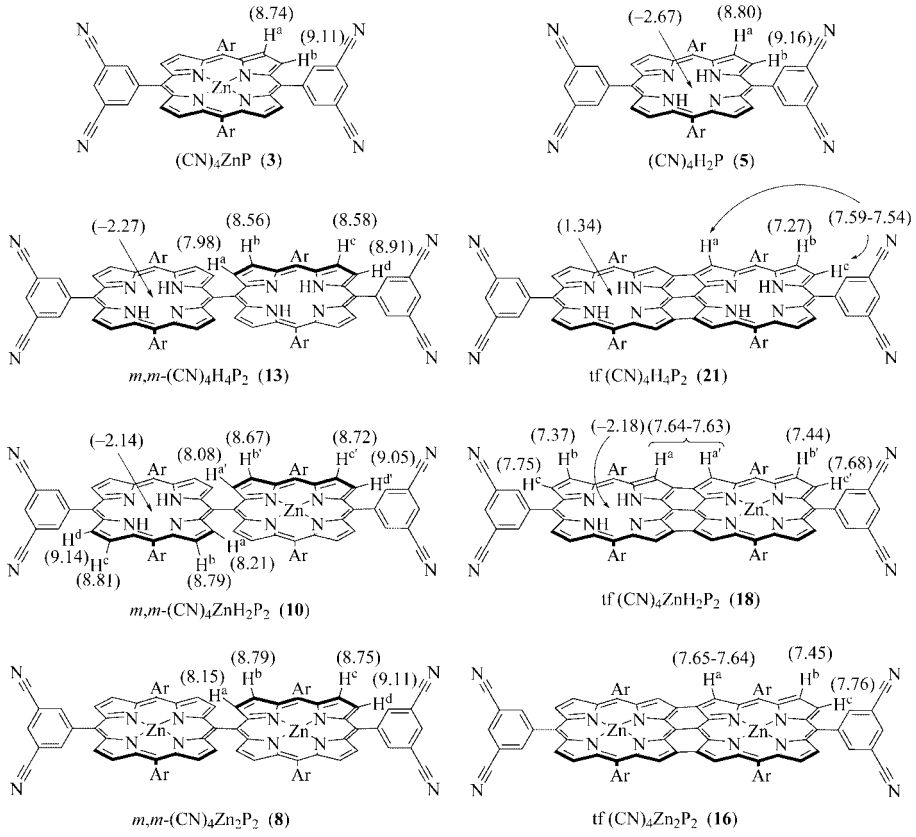

Figure 2. Selected ^{1}H NMR (300 MHz) spectroscopic data of mono- and diporphyrins in $CDCl_3$. Ar = 3,5-bis(*tert*-butyl)phenyl.

Table 1. UV/Vis spectra recorded in $CHCl_3$ at 293 K.

Compounds Monoporphyrins		Soret bands[a]	*Q*-bands[a]
ZnP	**1**	422 (204600)	549 (8200), 586 (2200)
$(CN)_2$ZnP	**2**	422 (186300)	549 (7600), 587 (1300)
$(CN)_4$ZnP	**3**	427 (114500)	550 (5400), 591 (1100)
$(CN)_4$CuP	**4**	423 (111200)	542 (5700), 577 (1000)
$(CN)_4H_2P$	**5**	426 (117600)	519 (5400), 554 (2400), 593 (1800), 649 (1300)
meso,*meso*-Diporphyrins			
Zn_2P_2	**6**	418 (347900), 457 (290400)	559 (70800), 595 (9700)
$(CN)_2Zn_2P_2$	**7**	424 (245700), 461 (240000)	565 (54300), 611 (1530)
$(CN)_4Zn_2P_2$	**8**	430 (137000), 460 (182500)	556 (39400), 637 (2300)
$(CN)_4Cu_2P_2$	**9**	419 (98600), 453 (107800)	551 (28500)
$(CN)_4ZnH_2P_2$	**10**	423 (166500), 457 (160000)	522 (24000), 556 (31400), 596 (11300), 653 (4500)
$(CN)_4CuH_2P_2$	**11**	421 (66000), 454 (63800)	522 (9300), 548 (12500), 593 (3700), 652 (1400)
$(CN)_4ZnCuP_2$	**12**	422 (146500), 456 (155200)	557 (37600), 638 (1300)
$(CN)_4H_4P_2$	**13**	421 (210500), 456 (230000)	527 (53700), 563 (16500), 596 (17500), 655 (8400)
Triply fused diporphyrins			
Zn_2P_2	**14**	419 (113000)	528 (101600), 1068 (22900)
$(CN)_2Zn_2P_2$	**15**	422 (136000), 460 (45700)	565 (112200), 923 (17900), 1053 (30600)
$(CN)_4Zn_2P_2$	**16**	423 (79100) ,469 (29800)	568 (81600), 955 (11000), 1093 (17200)
$(CN)_4Cu_2P_2$	**17**	416 (39700)	562 (35700), 576 (36000), 669 (3100), 987 (8300)
$(CN)_4ZnH_2P_2$	**18**	424 (72700), 478 (47900)	570 (71300), 1066 (15200), 1124 (10800), 1158 (6300)
$(CN)_4CuH_2P_2$	**19**	415 (58100)	566 (59300), 712 (5500), 1015 (15200)
$(CN)_4ZnCuP_2$	**20**	418 (89100), 462 (36100)	567 (76500), 911 (11600), 1038 (16100)
$(CN)_4H_4P_2$	**21**	416 (85300), 476 (39300)	567 (94800), 705 (11100), 1045 (19300), 1079 (19700)

[a] λ_{max} /nm [eV] (ε, $M^{-1}cm^{-1}$).

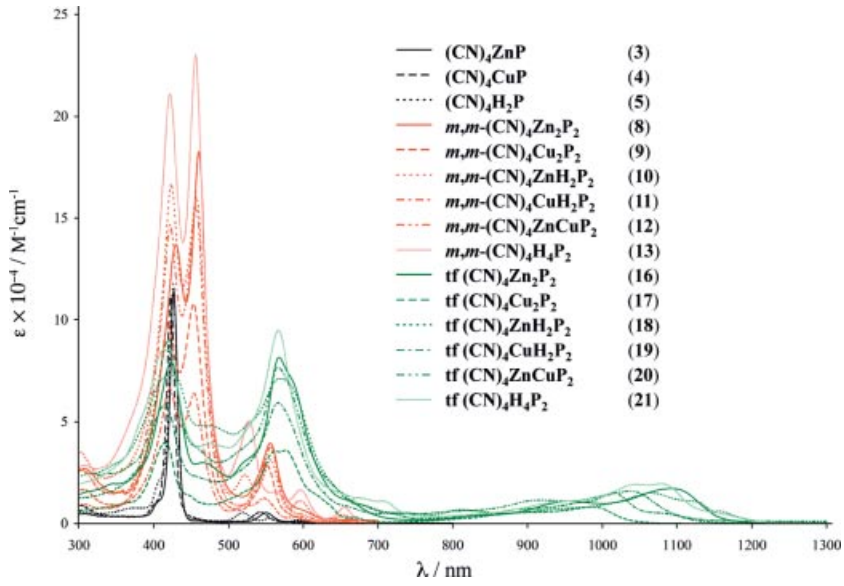

Figure 3. UV/Vis spectra of differentially metallated monoporphyrins **3**–**5**, *meso,meso*-diporphyrins **8**–**13**, and triply fused porphyrins **16**–**21** recorded in $CHCl_3$ at 293 K.

Table 2. Electrochemical reduction and oxidation potentials (V) vs. Fc/Fc^+ from differential pulse voltammograms of mono- and diporphyrins in CH_2Cl_2 (+ 0.1 M nBu_4NPF_6).

Compounds		Oxidation					Reduction				HOMO–LUMO gap[a]
		$E_{ox.1}$	$E_{ox.2}$	$E_{ox.3}$	$E_{ox.4}$	$E_{ox.5}$	$E_{red.1}$	$E_{red.2}$	$E_{red.3}$	$E_{red.4}$	
Monoporphyrins											
ZnP	**1**	0.31	0.59				–1.87	–2.26			2.18
$(CN)_2ZnP$	**2**	0.41	0.69				–1.66	–2.03	–2.24		2.07
$(CN)_4ZnP$	**3**	0.47	0.75				–1.65	–1.98	–2.34		2.12
$(CN)_4CuP$	**4**	0.68	0.95				–1.62	–2.00			2.30
$(CN)_4H_2P$	**5**	0.69	0.90				–1.47	–1.81			2.16
meso,meso-Diporphyrins											
Zn_2P_2	**6**	0.19	0.40	0.82	1.03		–1.86	–1.96	–2.28		2.05
$(CN)_2Zn_2P_2$	**7**	0.40[b]	0.49[b]	0.74[b]	0.80[b]	1.12	–1.71	–1.83	–2.18	–2.37	2.11
$(CN)_4Zn_2P_2$	**8**	0.43	0.53	0.80	0.99	1.16[b]	–1.68	–1.80	–2.09	–2.31[b]	2.11
$(CN)_4Cu_2P_2$	**9**	0.64	0.79				–1.64	–1.77			2.28
$(CN)_4ZnH_2P_2$	**10**	0.44	0.67	0.77	1.00		–1.62	–1.82	–2.06		2.06
$(CN)_4CuH_2P_2$	**11**	0.63	0.77				–1.62	–1.82			2.25
$(CN)_4ZnCuP_2$	**12**	0.46	0.66	0.77	0.95	1.21	–1.67[b]	–1.79[b]	–2.12		2.13
$(CN)_4H_4P_2$	**13**	0.63	0.77				–1.55	–1.66			2.18
Triply fused diporphyrins											
Zn_2P_2	**14**	0.03	0.25	0.75	1.03		–1.07	–1.33	–2.28		1.10
$(CN)_2Zn_2P_2$	**15**	0.01	0.38	0.89			–1.07	–1.26	–2.17		1.08
$(CN)_4Zn_2P_2$	**16**	0.13	0.33	0.86	1.08		–0.97	–1.21	–2.14		1.10
$(CN)_4Cu_2P_2$	**17**	0.40	0.73	1.16			–0.83	–1.08	–2.02		1.23
$(CN)_4ZnH_2P_2$	**18**	0.25	0.52	0.99			–1.00	–1.24	–2.19		1.25
$(CN)_4CuH_2P_2$	**19**	0.40	0.74	1.34			–0.83	–1.08	–2.04		1.23
$(CN)_4ZnCuP_2$	**20**	0.22	0.49	0.94			–0.92	–1.21	–2.13		1.14
$(CN)_4H_4P_2$	**21**	0.43	0.83				–0.76	–1.03			1.19

[a] Electrochemical HOMO–LUMO gap [eV]: $\Delta E = E_{ox.1} - E_{red.1}$. [b] Poorly defined potentials.

Although mechanistic details have been previously reported, these were concerned mainly with two families of dimeric cofacial diporphyrins with non-electroactive centers (Zn, Cu, 2 H), either covalently linked by two amide bridges or by a single polyaromatic bridge ("Pacman" family). Our studies of dimeric porphyrins include direct lateral connec-

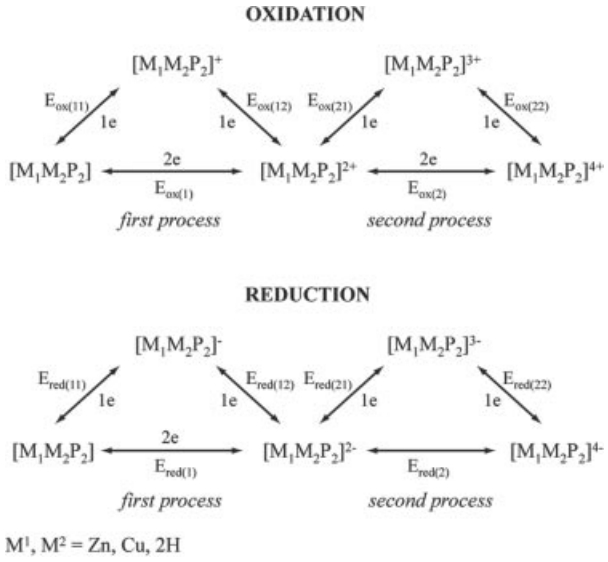

Scheme 5. General redox pathway for the oxidation or reduction of the diporphyrin rings.

tion between two porphyrins arraying them in biaryl-type (*meso*,*meso*) or planar (triply fused) orientation and guaranteeing maximum metal ion-metal ion interaction.[31]

Electrochemical Behavior of Monoporphyrins

Redox potentials were found to be better defined in DPV experiments due to peak overlap and/or irreversibility observed by CV. In the present discussion DPV results are utilized, therefore the redox potentials do not necessarily correspond to $E_{1/2}$ values. The DPVs of the monoporphyrins are shown in Figure 4a. All derivatives feature two reversible 1e oxidation steps and one reversible 1e reduction wave. The second 1e reduction is irreversible for the Zn^{II} derivative, but reversible for the free-base and Cu^{II} porphyrins.

The *meta*-CN groups on the *meso*-phenyl rings exert a pronounced σ-acceptor effect, leading to significant shifts in the redox potentials. Upon changing from ZnP (**1**) to $(CN)_2$ZnP (**2**) and to $(CN)_4$ZnP (**3**), the first reduction potential shifts anodically from –1.87 to –1.66 V and to –1.65 V, respectively. Correspondingly, oxidation becomes more difficult in this sequence (+0.31 → +0.41 → +0.47 V). The free-base porphyrin $(CN)_4H_2P$ (**5**; –1.47 V) is more readily reduced compared to the Zn^{II} (**3**; –1.65 V) and the Cu^{II} (**4**; –1.62 V) derivatives. On the other hand, the first oxidation of Zn^{II} porphyrin **3** (+0.47 V) is facilitated as compared to the corresponding electron transfer from the Cu^{II} (**4**; +0.68 V) or the free-base (**5**; +0.69 V) porphyrin. These observations are in agreement with previously reported data.[9b,14c,15c,29c–29f]

Electrochemical Behavior of *meso*,*meso*-Linked Diporphyrins

The DPVs are shown in Figure 4b and the measured redox potentials are listed in Table 2. As a general trend, the singly linked diporphyrins show similar behavior to that exhibited by the two individual macrocycles connected in an orthogonal, biaryl-type fashion. Three, and in some cases even four 1e reductions, as well as four to five 1e oxidations are observed, mirroring the doubling of the number of electroactive chromophores as compared to the monoporphyrins.

Similar to the monoporphyrin series, the exchange of the peripheral *tert*-butyl donor for CN acceptor groups shifts the potentials anodically from –1.86 V (*m*,*m*-Zn_2P_2, **6**) to –1.68 V [*m*,*m*-$(CN)_4Zn_2P_2$, **8**] and from +0.19 V to +0.43 V, respectively.

The bis(zinc) and bis(copper) derivatives *m*,*m*-$(CN)_4Zn_2P_2$ (**8**) and *m*,*m*-$(CN)_4Cu_2P_2$ (**9**), as well as the hybrid systems *m*,*m*-$(CN)_4ZnH_2P_2$ (**10**), *m*,*m*-$(CN)_4CuH_2P_2$ (**11**), and *m*,*m*-$(CN)_4ZnCuP_2$ (**12**) undergo the first two to three reduction steps at very similar potentials (Table 2). In

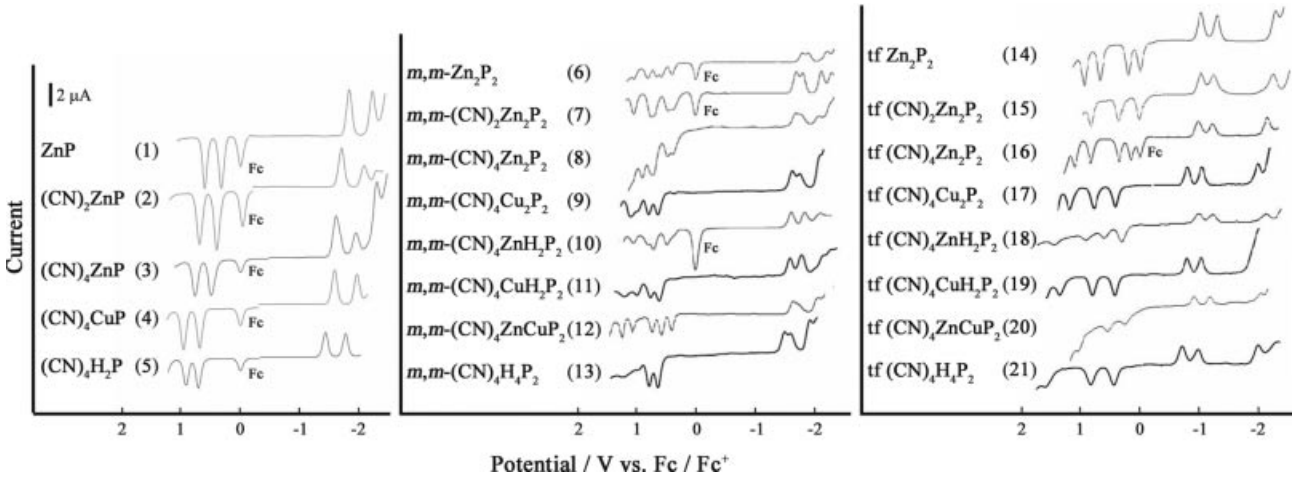

Figure 4. a) DPVs of porphyrin monomers **1**–**5**; b) *meso*,*meso*-linked diporphyrins **6**–**13**; and c) triply fused diporphyrins **14**–**21**.

comparison, the first two 1 e reduction steps of free-base *m*,*m*-$(CN)_4H_4P_2$ (**13**) are shifted anodically.

The potential for the first 1e oxidations of the zinc derivatives *m*,*m*-$(CN)_4Zn_2P_2$ (**8**), *m*,*m*-$(CN)_4ZnH_2P_2$ (**10**), and *m*,*m*-$(CN)_4ZnCuP_2$ (**12**) vary only slightly (first: +0.43 to +0.46 V; third: +0.77 to +0.80 V; fourth: +0.95 to +1.00 V), with the exception of the second, which is facilitated for Zn_2 derivative **8** (+0.53 V) as compared to the hybrid systems **10** (+0.67 V) and **12** (+0.66). In comparison, the first and second oxidation potentials of *m*,*m*-$(CN)_4Cu_2P_2$ (**9**), *m*,*m*-$(CN)_4CuH_2P_2$ (**11**) and metal-free *m*,*m*-$(CN)_4H_4P_2$ (**13**) are shifted anodically to 0.64 and 0.79 V (**9**) and 0.63 and 0.77 V (**11**, **13**), respectively, near the region of the second and third oxidation potentials of the zinc derivatives **8**, **10**, and **12**.

Accordingly, the fact that Zn^{II} monoporphyrin **3** is much easier to oxidize than Cu^{II} monoporphyrin **4** and free-base analog **5**, is consistent with the relative anodic shift of zinc(II)-containing *meso,meso*-linked diporphyrins **8**, **10**, and **12** as opposed to the corresponding zinc-free **9**, **11**, and **13**. Also, this may explain the facilitated second oxidation of the bis(zinc) derivative **8** with respect to monozinc diporphyrins **10** and **12**.

The fact that free-base derivative **5** is much easier to reduce than metallated **3** and **4**, is consistent with the easier reduction of the free-base derivative *m*,*m*-$(CN)_4H_4P_2$ (**13**).

One issue to consider is whether a metal-centered redox process occurs in the Cu^{II} porphyrin systems. There are only a few publications reporting the electrochemistry of copper porphyrins, which are mainly concerned with the electrochemical processes of the porphyrin ring.[32] Moreover, these reports are not consistent. Kadish et al. and Arnold et al. suggested that Cu^{II} porphyrin derivatives undergo only porphyrin ring-centered electrode reactions.[32a,32b] However, other electrochemical studies provide evidence for redox reactions of the Cu^{II}/Cu^{I} couple of Cu^{II} porphyrin derivatives.[32c,32d] By comparing the electrochemical behavior of *m*,*m*-$(CN)_4ZnCuP_2$ (**12**) and tf$(CN)_4$-$ZnCuP_2$ (**20**) with that of monomer $(CN)_4CuP$ (**4**) it can be concluded that none of the redox waves observed are Cu centered.

Electronic coupling between the two porphyrin rings in the singly linked dimers is also apparent from the peak splitting of the (partially overlapping) reduction and oxidation waves, i.e. the first and second electron transfers, which are centered on the two porphyrin rings, occur at different potentials. However, the CVs and DPVs of the triply fused dimers show a much more pronounced splitting due to the enhanced electronic coupling resulting from the full delocalization over the two porphyrin nuclei.[5c,5d,14a,15c,16]

Electrochemical Behavior of Triply Bridged Diporphyrins

In contrast to the rather poorly defined, overlapping redox waves of the singly linked dimers, the redox waves of the triply fused systems are perfectly defined and reversible, as a result of the larger splitting between successive processes (Figure 4c). In general within the limits of the potential window of the solvent (CH_2Cl_2), two to three nicely separated 1e reduction waves and two to four 1e oxidation waves are observed by CV and DPV. We define the value of the potential difference, $\Delta E_{ox} = E_{ox(12)} - E_{ox(11)}$, where $E_{ox(11)}$ and $E_{ox(12)}$ represent split potentials for the first oxidation and $\Delta E_{red} = |E_{red(12)} - E_{red(11)}|$, where $E_{red(12)}$ and $E_{red(11)}$ represent split potentials for the first reduction. Interestingly, the peak splitting values of the triply fused diporphyrins are strongly affected by the incorporation of the CN groups. Thus ΔE_{ox} (CV) increases from 200 (no CN, **21**) to 380 mV (2 CN, **23**), then decreases again to 200 mV (4 CN, **16**). The ΔE_{red} values are 260 (**21**), 190 (**23**), and 240 mV (**16**). The dependence of the splitting on the attached cyano groups may be ascribed to the different distribution of the molecular orbitals.[33]

The split of the first oxidation and reduction processes of the *meso*,*meso*-linked $(CN)_4$ diporphyrins are almost the same, in the range of 0.10–0.23 V (Figure 4b). These values indicate some degree of electronic interaction between the two porphyrins. The triply fused $(CN)_4$ diporphyrins exhibit much larger differences, in the range 0.20–0.40 V and 0.24–0.29 V (Figure 4c), respectively, between the oxidation and reduction processes. This behavior is further evidence of the stronger interaction between the two porphyrin rings in the triply fused than in the *meso*,*meso*-linked diporphyrins.

The electrochemical HOMO–LUMO gaps reveal another important difference between monoporphyrins and the two series of linked dimers.[5b–5d] Whereas the electrochemical gap in $(CN)_4ZnP$ (**3**) is 2.12 eV and is not lowered much upon changing to *m*,*m*-$(CN)_4Zn_2P_2$ (**8**; 2.11 eV), it is lowered to 1.10 eV in tf $(CN)_4Zn_2P_2$ (**16**). The lowered gap in triply fused **16** as compared to singly bridged **8** is a result of both a large anodic shift of the first reduction potential (710 mV) and a substantial cathodic shift of the first oxidation potential (300 mV). Similarly large reductions of the electrochemical gap can be calculated by comparing the DPV data (Table 2) of other related *meso*,*meso*-linked and triply fused systems. The low electrochemical gaps are a direct result of the more extensive π-conjugation in the planar triply fused dimers.

Introducing two peripheral CN groups into the triply fused systems hardly affects the first reduction and oxidation potentials as observed in the CV comparison between arylated **14** (–1.07; +0.03) and dicyano derivative **15** (–1.07; +0.01). Upon introduction of two additional CN groups in **16**, however, substantial potential shifts are observed, when compared to the dicyano derivative **15**. The reduction becomes facilitated by 90 mV (–0.97 V) and the oxidation becomes more difficult by 130 mV (+0.13 V).

Trends similar to those observed for the *meso*,*meso*-linked series become apparent when observing the influence of the metal ion centers. The values for the first and second oxidation potentials for the bis(copper) derivative *m*,*m*-$(CN)_4Cu_2P_2$ (**9**) are shifted anodically by 10 and 20 mV, respectively, as compared to the other zinc free diporphyrins **11** and **13**. There is a small anodic shift for tf $(CN)_4$-

Cu_2P_2 (**17**) and tf $(CN)_4CuH_2P_2$ (**19**, both +0.40 V) of 30 mV when compared to tf $(CN)_4H_4P_2$ (**21**, +0.43 V) for the first oxidation potential. There is also a similar shift for tf $(CN)_4Cu_2P_2$ (**17**, +0.73 V) of 10 mV when compared to tf $(CN)_4CuH_2P_2$ (**19**, +0.74) for the second oxidation potential. However, there is a larger anodic shift of 90 mV for the second 1e oxidation process when comparing the copper free-base hybrid **19** (+0.74 V) to metal-free **21** (+0.83 V).

Significantly lower first and second oxidation potentials are found for the zinc containing series tf $(CN)_4Zn_2P_2$ (**16**), tf $(CN)_4ZnH_2P_2$ (**18**) and tf $(CN)_4ZnCuP_2$ (**20**), reflecting the easier oxidation of zinc porphyrins already observed in the monoporphyrin and the *meso*,*meso*-linked diporphyrin series. As before there is a small anodic shift of 30 mV each for the first and second oxidation potential when comparing tf $(CN)_4ZnCuP_2$ (**20**) with the copper-free tf $(CN)_4ZnH_2P_2$ (**18**). The same trend of a slightly facilitated oxidation of copper porphyrins compared to the free-base, is observed for **18** with respect to tf $(CN)_4Zn_2P_2$ (**16**).

The reduction potentials of triply fused diporphyrins also show similar tendencies, when compared to the *meso*,*meso*-linked diporphyrins. The first and second reduction potentials of tf $(CN)_4Cu_2P_2$ (**17**) and tf $(CN)_4CuH_2P_2$ (**19**) are equal. There is an anodic shift of 70 and 50 mV, respectively, for the first and the second reduction potential when compared to the metal-free tf $(CN)_4H_4P_2$ (**21**). Zinc-containing diporphyrins **16**, **18**, and **20** show a much more difficult reduction, with tf $(CN)_4ZnH_2P_2$ (**18**) being the hardest to reduce.

Conclusions

A novel series of biaryl-type *meso*,*meso*-linked and planar triply fused diporphyrin arrays, featuring different numbers of CN groups attached to peripheral *meso*-aryl groups and bound to different metal ions (Cu^{II}, Zn^{II}), were prepared and their electronic properties investigated by UV/Vis spectroscopy and electrochemistry. The corresponding monoporphyrins were also studied as controls. Electronic communication between the two macrocycles is obviously strongest in the triply fused arrays with their extended π-chromophores. Whereas the electrochemical HOMO–LUMO gaps are essentially the same for the monoporphyrins (2.07–2.18 eV) and the *meso*,*meso*-linked arrays (2.05–2.28 eV), the gaps in the triply fused systems are reduced drastically by ca. 1 eV to values between 1.08 and 1.25 eV. This reduction of the HOMO–LUMO gap is enhanced upon a further increase in the number of fused porphyrin moieties.[4] The electrochemical behavior of the triply fused porphyrin dimers is significantly different from that of their corresponding, singly linked porphyrin dimers. In contrast with the typical poorly defined redox behavior of singly linked porphyrin dimers, the triply fused dimers display reversible redox behavior. Apparent redox splitting is observed for triply fused porphyrin dimers, which arises as a consequence of the improved electronic coupling resulting from full delocalization. However, singly linked porphyrin dimers exhibit an obvious overlap of one-electron steps for both reduction and oxidation. In all systems, the introduction of peripheral CN groups shifts the redox potentials, facilitating reduction and rendering oxidation more difficult.

Changing the metal ions proved to have a crucial influence on the redox potentials and the electrochemical gaps of all porphyrins investigated. In the monoporphyrin series, the Cu^{II} derivative **5** has the largest gap (2.30 eV), whereas the gaps in the Zn^{II} (**1**) and the free-base derivative (**4**) are reduced to 2.12 and 2.16 eV, respectively. This gap reduction mainly results from a greater ease of oxidation of the Zn^{II} and a facilitated reduction of the free-base porphyrin. This is also observed for the *meso*,*meso*-linked $(CN)_4$ systems, where the mixed-zinc/free-base diporphyrin **10** has the lowest gap (2.06 eV). Bis(copper) derivative **9** has the largest gap of the series (2.28 eV), with Cu monoporphyrin **4** being both relatively difficult to oxidize and to reduce. The actual decrease in the gaps for the *meso*,*meso*-$(CN)_4$ series is as follows: ZnH_2 (2.06 eV) < Zn_2 (2.11 eV) < ZnCu (2.13 eV) < H_4 (2.18 eV) < CuH_2 (2.25 eV) < Cu_2 (2.28 eV) reflecting the above-mentioned effects.

Notably, the effects of the metal ions on reduction potentials and the electrochemical gaps of the triply fused diporphyrins differ strongly from those seen in the monoporphyrins and *meso*,*meso*-linked diporphyrins. In the triply fused $(CN)_4M^1M^2P_2$ series, the order for the electrochemical gap is Zn_2 (1.10 eV) < ZnCu (1.14 eV) < H_4 (1.19 eV) < CuH_2, Cu_2 (1.23 eV) < ZnH_2 (1.25 eV). The Zn_2 diporphyrin possesses the smallest gap due to the easiest oxidation in the triply fused series. There is a substantial decrease of the first reduction potential of CuH_2 and Cu_2 compounds, which is not observed in the *meso*,*meso* series. This makes up for their more difficult oxidation compared to zinc containing diporphyrins. ZnH_2 turned out to have the biggest gap of the series. Unlike the *meso*,*meso* series, there seems to be no ease of reduction resulting from the free-base macrocycle; in fact, this dimer exhibits the highest first reduction potential of the triply fused series. It is important to emphasize that the influence of metal ions in the triply fused systems cannot be explained on the basis of the redox properties of the corresponding monoporphyrins!

This systematic electrochemical study reveals that electronic coupling in porphyrin arrays can be tuned by changing the connection mode, central metal, and attaching mode. This finding warrants a more extensive investigation of metal ion effects on the optical and electronic properties of triply fused oligoporphyrin arrays introduced by the Osuka group, which clearly are among the most exceptional advanced materials reported in recent years. Also, an investigation of the interactions of differentially metallated oligoporphyrin arrays with covalently linked fullerenes represents a worthwhile future endeavor, which will be pursued by the authors of this paper.

Experimental Section

Materials and General Methods: Chemicals were purchased from Acros, Aldrich, and Fluka and used as received. THF was distilled

from Na/benzophenone. Toluene (PhMe) was distilled from CaH_2. All porphyrin reactions were carried under an inert atmosphere by applying a positive pressure of N_2. Compounds **1**,[22] **2**,[23] **6**,[24] **7**,[5b,5d] **14**,[25] **15**,[5b,5d] and **22**[5b,5d] were prepared according to literature reports. Column chromatography was carried out using Fluka silica gel 60 (SiO_2; 230–400 mesh, particle size 0.040–0.063) or Fluka aluminium oxide (alumina; particle size 0.050–0.150, pH 7.0 ± 0.5). Melting points (M.p.) for all compounds except **9**, **11**, **13**, **17**, **19**, and **21** were measured in open capillaries with a Büchi Melting Point B540 apparatus and are uncorrected. Thermal analysis was performed for compounds **9**, **11**, **13**, **17**, **19**, and **21** as an estimation of the exact melting points by differential scanning calorimetry (DSC) with a DSC822^e (Mettler Toledo, Greifensee, Switzerland) equipped with an intracooler. Measurements were performed under N_2 and cooling, as well as at heating rates of 10 °C/min. The curves were not reversible, however there was no decomposition cognizable by ^{1}H NMR and FT-MALDI. It is yet unclear if the values indicated as M.p. are actually melting or decomposition temperatures. ^{1}H NMR and ^{13}C NMR spectra were measured on Varian Gemini 300 MHz spectrometers. Chemical shifts are reported in ppm downfield from $SiMe_4$ using the solvent's residual signal as an internal reference. Infrared spectra (IR) were recorded with a Perkin–Elmer FT1600 spectrometer or a Perkin–Elmer Spectrum BX II. UV/Vis spectra were recorded with a Varian CARY-5 or Varian CARY-500 spectrophotometer. The spectra were measured in $CHCl_3$ in a quartz cuvette of 1 cm length; λ_{max} [nm] (ε [$M^{-1}cm^{-1}$]); shoulders: sh. EI mass spectra were measured at 70 eV with a Hitachi-Perkin–Elmer VG-TRIBRID spectrometer. High-resolution (HR) FT-MALDI spectra (only the monoisotopic peak is reported) were measured with an Ionspec Fourier Transform instrument with 2,5-dihydroxybenzoic acid (DHB), 3-hydroxypicolinic acid (3-HPA) or *trans*-2-[3-(4-*tert*-butylphenyl)-2-methylprop-2-enylidene]malononitrile (DCTB) in MeOH/H_2O as matrix, and the compound in CH_2Cl_2 (two layer technique).

Electrochemistry: All electrochemical measurements were performed in re-distilled CH_2Cl_2 (degassed with Ar) with 0.1 M nBu$_4$NPF$_6$ as the supporting electrolyte on a CHI 660 Electrochemical Workstation (CH Instruments Inc, Austin, Texas). The supporting electrolyte, nBu$_4$NPF$_6$ (Aldrich, 98%), was recrystallized three times from ethanol and dried under vacuum for 24 h prior to use. The compounds were also dried under vacuum for 2 h prior to use. For all samples, except the ones mentioned below, a platinum wire was employed as the counter electrode. A silver wire was used as the reference. Ferrocene (Fc) was added as an internal reference, and all potentials were referenced relative to the Fc/Fc$^+$ couple. A glassy carbon electrode (CHI, 3 mm in diameter), polished with 0.3 μm aluminum paste and ultrasonicated in deionized water and CH_2Cl_2 bath, was used as the working electrode. Scan rates for cyclic voltammetry (CV) and differential pulse voltammetry (DPV) were 100 and 4 mV/s, respectively. For DPV measurements, the amplitude was 50 mV and the pulse width was 0.05 s. For samples **9**, **11**, **13**, **17**, **19**, and **21**, voltammetric experiments were performed using a potentiostat/galvanostat Model CHI660A (CH Instruments Electrochemical Workstation) with a three-electrode cell placed in a Faraday cage. The working electrodes consisted of a platinum disk (Bioanalytical Systems, Inc.) with a diameter of 1.0 mm. The surface of the electrode was polished using extra fine carborundum paper (Buehler) followed by 0.3 μm alumina and 0.25 μm diamond polishing compound (Metadi II, Buehler). Next, the electrode was sonicated in water in order to remove the traces of alumina from the metal surface, washed with water, and dried. A silver wire immersed in 0.01 mol dm^{-3} silver nitrate and 0.09 mol dm^{-3} (nBu)$_4$NPF$_6$ in acetonitrile and separated from the analysis solution by a ceramic tip (Bioanalytical System Inc.) served as the reference electrode. The silver hexafluorophosphate solution was replaced daily, because of the instability of Ag^+ to photoreduction. The stability of the reference electrode was examined by recording the ferrocene oxidation potential in the solvent studied as a function of time. The formal potential of the ferrocene-ferricenium system was found to be stable for about 12 h. The counter electrode was made from platinum mesh (0.25 mm). The solution was deaerated for 20 min with Ar prior to the electrochemical measurements. All experiments were performed at room temperature. All potentials obtained from the DPV were corrected using the formula $E_{max} = E_{1/2} + \Delta E/2$, where ΔE is the pulse amplitude.

{μ-[10,10′,20,20′-Tetrakis(3,5-di-*tert*-butylphenyl)-15,15′-bis(3,5-dicyanophenyl)-5,5′-biporphyrinato(4-)-κ*N*^{21},κ*N*^{22},κ*N*^{23},κ^{24}:κ*N*$^{21'}$,κ*N*$^{22'}$,κ*N*$^{23'}$,κ*N*$^{24'}$]}dizinc(II) [*m*,*m*-(CN)$_4$Zn$_2$P$_2$ (8)]

Method A: A saturated solution of $Zn(OAc)_2$ in MeOH was added to a solution of **10** (25 mg, 1.5×10^{-2} mmol) in $CHCl_3$, and the resulting mixture was heated to reflux for 3 h in the dark to yield **7** (26 mg, quant.) as a brown solid.

Method B: To a solution of **6** (100 mg, 1.1×10^{-1} mmol) in $CHCl_3$ (30 mL) was added a solution of $AgPF_6$ (60 mg, 2.4×10^{-1} mmol) in CH_3CN (3 mL), and the mixture heated to reflux for 3 h. More $AgPF_6$ (60 mg, 2.4×10^{-1} mmol) was added and heating to reflux was continued for 18 h. The mixture was washed with water, the organic layer dried (Na_2SO_4), and the solvent evaporated. The resulting brown solid was dissolved in $CHCl_3$ (20 mL) and treated with a solution of $Zn(OAc)_2$ (1 g, 5.5 mmol) in MeOH (20 mL). After stirring at 20 °C for 2 h, the mixture was washed with water and dried (Na_2SO_4). Evaporation and flash chromatography (SiO_2; CH_2Cl_2/hexane, 4:1) afforded **7** (78 mg, 80%) as a brown solid. M.p. >300 °C. ^{1}H NMR (300 MHz, $CDCl_3$): δ = 9.11 (d, J = 4.5 Hz, 4 H), 8.83 (d, J = 0.7 Hz, 4 H), 8.79 (d, J = 5.1 Hz, 4 H), 8.75 (d, J = 4.5 Hz, 4 H), 8.40 (t, J = 0.7 Hz, 2 H), 8.15 (d, J = 5.1 Hz, 4 H), 8.08 (d, J = 1.8 Hz, 8 H), 7.73 (t, J = 1.8 Hz, 4 H), 1.46 (s, 72 H) ppm. ^{13}C NMR (75.41 MHz, $CDCl_3$): δ = 167.99, 148.89, 132.68, 131.11, 130.40, 130.04, 129.03, 121.21, 116.70, 112.70, 35.05, 31.90 ppm. IR (neat): $\tilde{\nu}$ = 2957 (m), 2923 (m), 2856 (m), 2236 (w), 1722 (m), 1590 (m), 1516 (w), 1458 (m), 1426 (w), 1392 (w), 1362 (m), 1334 (m), 1279 (s), 1226 (m), 1120 (m), 1068 (s), 1009 (s), 951 (m), 934 (m), 883 (m), 822 (m), 790 (s), 732 (m), 713 (m), 688 (m) cm^{-1}. UV/Vis ($CHCl_3$): λ (ε, $M^{-1}cm^{-1}$) = 430 (137000), 460 (182500), 556 (39400), 637 (2300) nm. HR-MALDI-MS (DCTB mix): calcd. for $C_{112}H_{106}N_{12}Zn_2^+$ [M]$^+$ 1746.72; found 1746.72.

{μ-[10,10′,20,20′-Tetrakis(3,5-di-*tert*-butylphenyl)-15,15′-bis(3,5-dicyanophenyl)-5,5′-biporphyrinato(4–)-κ*N*^{21},κ*N*^{22},κ*N*^{23},κ^{24}:κ*N*$^{21'}$,κ*N*$^{22'}$,κ*N*$^{23'}$,κ*N*$^{24'}$]}dicopper(II) [*m*,*m*-(CN)$_4$Cu$_2$P$_2$ (9)]: Diporphyrin **13** (18 mg, 1.1×10^{-2} mmol) in $CHCl_3$ (3 mL) and $Cu(OAc)_2$ in MeOH (3 mL) was heated to reflux for 30 h. $CHCl_3$ was added, and the mixture was washed with water (3×), dried with Na_2SO_4, and the solvent evaporated. Purification over a short column (SiO_2; CH_2Cl_2/cyclohexane, 9:1) afforded **9** as a violet solid (20 mg, quant.). M.p. 380 °C. IR (neat): $\tilde{\nu}$ = 2923 (s), 2853 (s), 2360 (w), 2324 (w), 2237 (w), 2052 (w), 1981 (w), 1809 (w), 1682 (w), 1591 (m), 1538 (w), 1456 (m), 1393 (w), 1362 (m), 1338 (m), 1291 (m), 1248 (m), 1222 (w), 1209 (w), 1074 (m), 1001 (s), 950 (m), 930 (m), 882 (m), 824 (m), 796 (s), 761 (m), 714 (s), 688 (m), 630 (w) cm^{-1}. UV/Vis ($CHCl_3$): λ (ε, $M^{-1}cm^{-1}$) = 419 (98600), 453 (107800), 551 nm (28500). HR-MALDI-MS (3-HPA): calcd. for $C_{112}H_{106}Cu_2N_{12}^+$ [M]$^+$ 1744.73; found 1744.72.

[10,10′,20,20′-Tetrakis(3,5-di-*tert*-butylphenyl)-15,15′-bis(3,5-dicyanophenyl)-5,5′-biporphyrinato(2–)-κN^{21},κN^{22},κN^{23},κ^{24}]zinc(II) [*m*,*m*-(CN)$_4$ZnH$_2$P$_2$ (10)]: Compounds **26** (27 mg, 2.8×10^{-2} mmol) and **27** (28 mg, 2.8×10^{-2} mmol), together with Cs_2CO_3 (14 mg, 4.2×10^{-2} mmol) and [Pd(PPh$_3$)$_4$] (4 mg, 3.2×10^{-3} mmol) were dissolved in a mixture of dry DMF (1.8 mL) and dry PhMe (3.5 mL). The solution was deoxygenated via three freeze–pump–thaw cycles, and the resulting mixture was heated to 80 °C for 3 h under N_2. Water was added, and the mixture was extracted with $CHCl_3$. The organic layer was dried (Na_2SO_4), passed through a short column (SiO_2), and the solvents evaporated. Chromatography (SiO_2; CH_2Cl_2/cyclohexane, 2:1) gave **10** as red solid. Yield 46%. M.p. >300 °C. ^{1}H NMR (300 MHz, $CDCl_3$): δ = 9.14 (d, J = 4.5 Hz, 2 H), 9.05 (d, J = 4.5 Hz, 2 H), 8.86 (d, J = 3.2 Hz, 4 H), 8.81 (d, J = 4.5 Hz, 2 H), 8.79 (d, J = 4.5 Hz, 2 H), 8.72 (d, J = 4.5 Hz, 2 H), 8.67 (d, J = 4.5 Hz, 2 H), 8.43 (m, 2 H), 8.21 (d, J = 4.5 Hz, 2 H), 8.11 (s, 2 H), 8.08 (d, J = 4.5 Hz, 2 H), 7.76 (s, 4 H), 1.48 (s, 72 H), –2.14 (s, 2 H) ppm. ^{13}C NMR (75.41 MHz, $CDCl_3$): δ = 154.88, 151.14, 150.57, 148.85, 148.64, 146.28, 145.72, 141.10, 140.41, 140.28, 140.17, 134.24, 133.39, 132.85, 130.35, 129.80, 129.65, 124.24, 123.30, 121.28, 121.08, 119.44, 116.96, 116.87, 115.02, 113.84, 112.77, 112.56, 35.13, 31.79 ppm. IR (neat): $\tilde{\nu}$ = 2960 (m), 2902 (m), 2342 (w), 2237 (w), 2099 (w), 1801 (w), 1684 (m), 1589 (m), 1525 (w), 1475 (m), 1425 (m), 1393 (m), 1361 (m), 1287 (m), 1259 (s), 1066 (s), 1000 (s), 978 (m), 951 (m), 933 (m), 914 (m), 899 (m), 881 (m), 800 (s), 713 (m), 687 (m), 668 (m) cm^{-1}. UV/Vis ($CHCl_3$): λ (ε, M^{-1}cm^{-1}) = 423 (166500), 457 (160000), 522 (24000), 556 (31400), 596 (11300), 653 (4500) nm. HR-MALDI-MS (DCTB mix): calcd. for $C_{112}H_{108}N_{12}Zn^+$ [M]$^+$ 1684.81; found 1684.81.

[10,10′,20,20′-Tetrakis(3,5-di-*tert*-butylphenyl)-15,15′-bis(3,5-dicyanophenyl)-5,5′-biporphyrinato(2–)-κN^{21},κN^{22},κN^{23},κ^{24}]copper(II) [*m*,*m*-(CN)$_4$CuH$_2$P$_2$ (11)]: Compounds **28** (16 mg, 1.6×10^{-2} mmol) and **26** (15 mg, 1.6×10^{-2} mmol), together with Cs_2CO_3 (8 mg, 2.4×10^{-2} mmol) and [Pd(PPh$_3$)$_4$] (4 mg, 3.2×10^{-3} mmol) were dissolved in a mixture dry DMF (1 mL) and dry PhMe (2 mL). After purging with N_2 for 2 h, the solution was heated to 80 °C for 5 h. The mixture was diluted with chloroform, washed with water (3×), and dried with Na_2SO_4. After filtration through a plug (SiO_2), the solvent was evaporated and column chromatography (SiO_2; CH_2Cl_2/cyclohexane, 3:1) afforded **11** as a violet solid (20 mg, 75%) Alternatively, the coupling was also conducted with compounds **29** and **30** (yield: 99%). M.p. 367 °C. IR (neat): $\tilde{\nu}$ = 3313 (w), 2924 (s), 2854 (m), 2237 (w), 2163 (w), 2051 (w), 1980 (w), 1654 (w), 1591 (m), 1560 (w), 1459 (m), 1363 (w), 1291 (w), 1008 (s), 796 (s), 761 (w), 714 (w), 689 (w) cm^{-1}. UV/Vis ($CHCl_3$): λ (ε, M^{-1}cm^{-1}) = 421 (66000), 454 (63800), 522 (9300), 548 (12500), 593 (3700), 652 (1400) nm. HR-MALDI-MS (3-HPA): calcd. for $C_{112}H_{108}Cu^+N_{12}$ [M]$^+$ 1683.81; found 1683.81.

{μ-[Tetrakis(3,5-di-*tert*-butylphenyl)-15,15′-bis(3,5-dicyanophenyl)-10,10′,20,20′-5,5′-biporphyrinato(4–)-κN^{21},κN^{22},κN^{23},κ^{24}:κ$N^{21'}$,κ$N^{22'}$,κ$N^{23'}$,κ$N^{24'}$]}-zinc(II)copper(II) [*m*,*m*-(CN)$_4$ZnCuP$_2$ (12)]: A saturated solution of $Cu(OAc)_2$ in MeOH was added to a solution of **10** (30 mg, 1.8×10^{-2} mmol) in $CHCl_3$, and the resulting mixture was heated to reflux for 3 h in the dark to yield **12** (31 mg, quant.) as a red-yellow solid. M.p. >300 C. IR (neat): $\tilde{\nu}$ = 2958 (m), 2925 (m), 2865 (m), 2324 (w), 2237 (w), 1727 (w), 1685 (s), 1591 (m), 1475 (m), 1458 (m), 1426 (m), 1406 (m), 1384 (s), 1362 (m), 1334 (m), 1283 (m), 1248 (m), 1208 (m), 1087 (m), 997 (s), 949 (m), 928 (m), 900 (m), 883 (m), 824 (m), 792 (m), 725 (m), 714 (m), 687 (m), 658 (m) cm^{-1}. UV/Vis ($CHCl_3$): 422 (146500), 456 (155200), 557 (37600), 638 (1300) nm. HR-MALDI-MS (DCTB mix): calcd. for $C_{112}H_{106}CuN_{12}Zn^+$ [M]$^+$ 1745.73; found 1745.72.

{μ-[Tetrakis(3,5-di-*tert*-butylphenyl)-15,15′-bis(3,5-dicyanophenyl)-10,10′,20,20′-5,5′-biporphyrinato(4-)-κN^{21},κN^{22},κN^{23},κ^{24}:κ$N^{21'}$,κ$N^{22'}$,κ$N^{23'}$,κ$N^{24'}$]} [*m*,*m*-(CN)$_4$H$_4$P$_2$ (13)]: Compound **8** (150 mg, 8.6×10^{-2} mmol) was dissolved in a 1:1 mixture of MeOH/conc. HCl and stirred briefly. After TLC confirmed completion of the reaction, saturated aqueous $NaHCO_3$ and CH_2Cl_2 were added and the mixture was washed with 2 N aqueous Na_2CO_3, followed by water. The organic phases were dried with $MgSO_4$ and the solvent evaporated to give **13** as a violet solid (139 mg, quant.). M.p. 358–363 °C. ^{1}H NMR (300 MHz, $CDCl_3$): δ = 8.91 (d, J = 4.8 Hz, 4 H), 8.72 (d, J = 1.5 Hz, 4 H), 8.58 (d, J = 4.8 Hz, 4 H), 8.56 (d, J = 4.8 Hz, 4 H), 8.31 (t, J = 1.5 Hz, 2 H), 7.98 (d, J = 4.8 Hz, 4 H), 7.96 (d, J = 1.8 Hz, 8 H), 7.63 (t, J = 1.8 Hz, 4 H), 1.34 (s, 72 H), –2.27 (s, 4 H) ppm. ^{13}C NMR (125.76 MHz, $CDCl_3$): δ = 149.20, 146.00, 140.67, 140.54, 134.64, 130.01, 123.63, 121.61, 118.80, 117.09, 114.22, 113.04, 35.22, 31.86 ppm. IR (neat): $\tilde{\nu}$ = 3316 (w), 2957 (m), 2923 (s), 2853 (m), 2238 (w), 2051 (w), 1981 (w), 1812 (w), 1683 (m), 1591 (m), 1560 (w), 1459 (m), 1428 (w), 1400 (w), 1362 (m), 1297 (w), 1259 (s), 1078 (w), 1016 (w), 980 (m), 965 (m), 930 (w), 914 (m), 882 (m), 799 (s), 735 (m), 715 (m), 686 (w), 641 (w) cm^{-1}. UV/Vis ($CHCl_3$): λ (ε, M^{-1}cm^{-1}) = 421 (210500), 456 (230000), 527 (53700), 563 (16500), 596 (17500), 655 (8400) nm. HR-MALDI-MS (3-HPA): calcd. for $C_{112}H_{110}N_{12}^+$ [M]$^+$ 1622.90; found 1622.90.

{μ-[5,5′,15,15′-Tetrakis(3,5-di-*tert*-butylphenyl)-10,10′-bis(3,5-dicyanophenyl)-18,18′:20,20′-dicyclo-2,2′-biporphyrinato(4-)-κN^{21},κN^{22},κN^{23},κ^{24}:κ$N^{21'}$,κ$N^{22'}$,κ$N^{23'}$,κ$N^{24'}$]}dizinc(II) [tf (CN)$_4$Zn$_2$P$_2$ (16)]

Method A: Sc(OTf)$_3$ (174 mg, 3.5×10^{-1} mmol) and DDQ (100 mg, 4.4×10^{-1} mmol) were added under N_2 to a solution of **8** (154 mg, 8.6×10^{-2} mmol) in dry PhMe (150 mL). The mixture was heated to reflux at 140 °C for 30 min. After cooling to 25 °C, the mixture was diluted with pyridine (5 mL), washed with H_2O (3×100 mL) and saturated aqueous NaCl (3×100 mL), dried with Na_2SO_4, and the solvent was evaporated in vacuo. Purification by repeated flash chromatography (SiO_2; CH_2Cl_2 containing 1% v/v Et_3N then Al_2O_3; cyclohexane/CH_2Cl_2, 98:2 containing 1% v/v Et_3N), followed by precipitation from $CHCl_3$ by dropwise addition of hexane, afforded **16** (154 mg, quant.).

Method B: Sc(OTf)$_3$ (400 mg. 8.1×10^{-1} mmol) and DDQ (200 mg, 8.8×10^{-1} mmol) were added under N_2 to a solution of **24** (254 mg, 2.9×10^{-1} mmol) in dry PhMe (150 mL). The mixture was heated to reflux at 140 °C for 30 min. After the workup (see above), **16** (235 mg, 89%) was obtained as a dark blue powder. M.p. >300 °C. ^{1}H NMR (300 MHz, $CDCl_3$): δ = 8.31 (d, J = 1.5 Hz, 4 H), 8.16 (t, J = 1.5 Hz, 2 H), 7.76 (d, J = 4.7 Hz, 4 H), 7.65–7.64 (m, 12 H), 7.45 (d, J = 4.7 Hz, 4 H), 7.34 (s, 4 H); 1.46 (s, 72 H) ppm. ^{13}C NMR (75.41 MHz, $CDCl_3$): δ = 154.14, 153.64, 151.32, 148.90, 139.36, 139.13, 136.06, 132.29, 130.76, 129.38, 128.68, 128.17, 126.95, 121.11, 116.60, 113.05, 109.80, 35.01, 31.72 ppm. IR (neat): $\tilde{\nu}$ = 2960 (m), 2923 (m), 2236 (w), 1791 (w), 1722 (m), 1697 (m), 1589 (m), 1477 (m), 1456 (m), 1423 (m), 1393 (m), 1379 (w), 1362 (w), 1343 (m), 1258 (s), 1200 (m), 1042 (s), 1018 (s), 951 (m), 942 (m), 898 (m), 880 (m), 790 (s), 739 (w), 714 (m), 687 (m), 667 (w) cm^{-1}. UV/Vis: 423 (79100), 469 (29800), 568 (81600), 955 (11000), 1093 (17200) nm. HR-MALDI-MS (DCTB mix): calcd. for $C_{112}H_{102}N_{12}Zn_2^+$ [M]$^+$ 1742.69; found 1742.69.

{μ-[Tetrakis(3,5-di-*tert*-butylphenyl)-10,10′-bis(3,5-dicyanophenyl)-5,5′,15,15′-18,18′:20,20′-dicyclo-2,2′-biporphyrinato(4-)-κN^{21},κN^{22},κN^{23},κ^{24}:κ$N^{21'}$,κ$N^{22'}$,κ$N^{23'}$,κ$N^{24'}$]}dicopper(II) [tf (CN)$_4$Cu$_2$P$_2$ 17];{μ-[5,5′,15,15′-Tetrakis(3,5-di-*tert*-butylphenyl)-10,10′-bis(3,5-dicyanophenyl)-18,18′:20,20′-dicyclo-2,2′-biporphyrinato(4-)-κN^{21},κN^{22},κN^{23},κ^{24}]}copper(II) [tf (CN)$_4$CuH$_2$P$_2$ (19)]: A solution

of **21** (40 mg, 2.5×10^{-2} mmol) in $CHCl_3$ (10 mL) and a saturated solution of $Cu(OAc)_2$ in MeOH (10 mL) were heated to reflux for 3 h. More $CHCl_3$ was added, and the mixture was washed ($3\times H_2O$), dried (Na_2SO_4), and the solvent was evaporated. Column chromatography (SiO_2; CH_2Cl_2/cyclohexane, 9:1) gave 43 mg of a mixture of **17** and **19**. The mixture was dissolved in CH_2Cl_2 (10 mL) and treated with DIEA. After being stirred at room temperature for 30 min, it was diluted with CH_2Cl_2 and washed ($3\times$ saturated aqueous $NaHCO_3$) and the organic layer was dried (Na_2SO_4) and the solvents evaporated. The residue was chromatographed (alumina; CH_2Cl_2/cyclohexane, 3:1 → CH_2Cl_2/EtOAc, 9:1) to obtain **17** (34 mg, 78% yield) and **31** (7.3 mg, 17% yield) as violet solids. Compound **31** was diluted in a solution of TFA (0.1 mL) in $CHCl_3$ (10 mL) and was stirred overnight at 20 °C. Subsequently, Et_3N (2 mL) was added dropwise, and the mixture was diluted with CH_2Cl_2, washed ($3\times H_2O$), the organic phase filtered through a plug (SiO_2), and the solvent evaporated to give **19** (7.2 mg, quant.) as a violet solid. Data for **17**: M.p. 322 °C. IR (neat): $\tilde{\nu}$ = 2958 (s), 2925 (s), 2857 (s), 2237 (m), 2051 (w), 1981 (w), 1803 (w), 1676 (w), 1676 (w), 1591 (s), 1506 (m), 1459 (m), 1425 (m), 1393 (m), 1348 (m), 1299 (m), 1258 (s), 1077 (s), 1009 (s), 953 (m), 942 (m), 882 (m), 793 (s), 715 (m), 689 (m), 664 (w), 630 (m) cm^{-1}. UV/Vis ($CHCl_3$): λ (ε, $M^{-1}cm^{-1}$) = 416 (39700), 562 (35700), 576 (36000), 669 (3100), 987 (8300) nm. HR-MALDI-MS (3-HPA): calcd. for $C_{112}H_{102}Cu_2N_{12}^+$ $[M]^+$ 1740.69; found 1740.69. Data for **19**: M.p. 345 °C. IR (neat): $\tilde{\nu}$ = 3351 (w), 2955 (s), 2923 (s), 2853 (s), 2349 (w), 2238 (w), 2163 (w), 2051 (w), 1981 (w), 1661 (m), 1632 (m), 1591 (m), 1523 (w), 1460 (m), 1426 (m), 1393 (m), 1362 (m), 1290 (m), 1248 (m), 1222 (w), 1072 (m), 1010 (m), 954 (w), 934 (w), 900 (w), 882 (w), 820 (m), 794 (m), 760 (w), 715 (m), 688 (w), 646 (w) cm^{-1}. UV/Vis ($CHCl_3$): 415 (58100), 566 (59300), 712 (5500), 1015 (15200). HR-MALDI-MS (3-HPA): calcd. for $C_{112}H_{104}CuN_{12}^+$ $[M]^+$ 1679.78; found 1679.88.

[5,5′,15,15′-Tetrakis(3,5-di-*tert*-butylphenyl)-10,10′-bis(3,5-dicyanophenyl)-18,18′:20,20′-dicyclo-2,2′-biporphyrinato(4-)-κN^{21},κN^{22},κN^{23},κ^{24}]zinc(II) [tf (CN)$_4$ZnH$_2$P$_2$ (18)]: $Sc(OTf)_3$ (170 mg, 3.4×10^{-1} mmol) and DDQ (85 mg, 3.4×10^{-1} mmol) were added under N_2 to a solution of **10** (90 mg, 5×10^{-2} mmol) in dry PhMe (50 mL). The mixture was heated to reflux at 140 °C for 3 h. After cooling to 25 °C, THF (25 mL) was added and stirring was continued for 1 h. The mixture was passed over a short column (Al_2O_3) and the solvent removed. The residue was purified by chromatography (SiO_2; cyclohexane/CH_2Cl_2, 1:5) to yield **18** (15 mg, 15%) as a dark purple solid. M.p. >300 °C. ^{1}H NMR (300 MHz, $CDCl_3$): δ = 8.32–8.30 (m, 4 H), 8.18–8.16 (m, 2 H), 7.75 (d, J = 4.5 Hz, 2 H), 7.68 (d, J = 5.4 Hz, 2 H), 7.64–7.63 (m, 12 H), 7.44 (d, J = 5.4 Hz, 2 H), 7.37 (d, J = 4.5 Hz, 2 H), 7.34 (s, 4 H), 1.46 (s, 72 H), –2.18 (s, 2 H) ppm. ^{13}C NMR (75.41 MHz, $CDCl_3$): δ = 154.88, 151.14, 150.57, 148.85, 148.64, 146.28, 145.72, 141.10, 140.41, 140.28, 140.17, 134.24, 133.39, 132.85, 130.35, 129.80, 129.65, 124.24, 123.30, 121.28, 121.08, 119.44, 116.96, 116.87, 115.02, 113.84, 112.77, 112.56 ppm. IR (neat): $\tilde{\nu}$ = 2961 (m), 2238 (w), 1593 (m), 1476 (s), 1393 (w), 1363 (m), 1345 (w), 1300 (m), 1266 (w), 1247 (m), 1225 (w), 1199 (s), 1074 (w), 1023 (m), 1001 (m), 943 (s), 900 (m), 881 (m), 826 (m), 791 (s), 724 (m), 716 (m), 696 (m), 658 (w) cm^{-1}. UV/Vis ($CHCl_3$): λ (ε, $M^{-1}cm^{-1}$) = 424 (72700), 478 (47900), 570 (71300), 1066 (15200), 1124 (10800), 1158 (6300) nm. HR-MALDI-MS (DCTB mix): calcd. for $C_{112}H_{108}N_{12}Zn^+$ $[M]^+$ 1680.78; found 1680.78.

{μ-[Tetrakis(3,5-di-*tert*-butylphenyl)-10,10′-bis(3,5-dicyanophenyl)-5,5′,15,15′-18,18′:20,20′-dicyclo-2,2′-biporphyrinato(4-)-κN^{21},κN^{22},κN^{23},κ^{24}:κ$N^{21'}$,κ$N^{23'}$,κ$N^{24'}$]}zinc(II)copper(II) [tf (CN)$_4$ZnCuP$_2$ (20)]: A saturated solution of $Cu(OAc)_2$ in MeOH was added to a solution of **18** (15 mg, 8.9×10^{-3} mmol) in $CHCl_3$, and the resulting mixture was heated to reflux for 3 h in the dark to yield **20** (15 mg, quant.) as a gray solid. M.p. >300 °C. IR (neat): $\tilde{\nu}$ = 2943 (m), 2925 (m), 2855 (m), 2310 (w), 2237 (w), 1737 (w), 1694 (s), 1595 (m), 1480 (m), 1459 (m), 1426 (m), 1411 (m), 1387 (s), 1362 (m), 1334 (m), 1298 (m), 1250 (m), 1218 (m), 1054 (m), 990 (s), 935 (m), 912 (m), 900 (m), 883 (m), 824 (m), 801 (m), 725 (m), 714 (m), 687 (m), 660 (m) cm^{-1}. UV/Vis ($CHCl_3$): λ (ε, $M^{-1}cm^{-1}$) = 418 (89100), 462 (36100), 567 (76500), 911 (11600), 1038 (16100) nm. HR-MALDI-MS (DCTB mix): calcd. for $C_{112}H_{102}CuN_{12}Zn^+$ $[M]^+$ 1741.69; found 1741.70.

{μ-[Tetrakis(3,5-di-*tert*-butylphenyl)-10,10′-bis(3,5-dicyanophenyl)-5,5′,15,15′-18,18′:20,20′-dicyclo-2,2′-biporphyrinato(4–)-κN^{21},κN^{22},κN^{23},κ^{24}:κ$N^{21'}$,κ$N^{22'}$,κ$N^{23'}$,κ$N^{24'}$]} [tf (CN)$_4$H$_4$P$_2$ (21)]: A solution of **16** (49 mg, 2.8×10^{-2} mmol) in MeOH/conc. HCl, 1:1 was stirred for 30 min. Then saturated aqueous $NaHCO_3$ and CH_2Cl_2 were added, and the mixture was washed with 2 N aqueous Na_2CO_3, followed by water. The organic phases were dried with $MgSO_4$ and the solvent evaporated to give **21** as a violet solid (45 mg, quant.). M.p. 325 °C. ^{1}H NMR (300 MHz, $CDCl_3$): δ = 8.22 (d, J = 1.5 Hz, 4 H), 8.08 (t, J = 1.5 Hz, 2 H), 7.59–7.54 (m, 20 H), 7.28 (d, J = 4.8 Hz, 4 H), 1.37 (s, 72 H), 1.34 (s, 4 H) ppm. ^{13}C NMR (125.76 MHz, $CDCl_3$): δ = 149.55, 144.32, 139.51, 138.90, 134.64, 128.54, 126.43, 121.78, 117.98, 117.20, 116.79, 113.57, 35.18, 31.86 ppm. IR (neat): $\tilde{\nu}$ = 3068 (w), 2953 (s), 2923 (s), 2855 (m), 2237 (m), 1728 (w), 1590 (m), 1558 (w), 1458 (m), 1414 (m), 1392 (w), 1361 (m), 1293 (w), 1247 (m), 1230 (m), 1176 (w), 1132 (w), 1079 (w), 1013 (w), 999 (w), 924 (m), 897 (w), 881 (w), 818 (m), 793 (s), 752 (w), 723 (s), 686 (m), 644 (m), 623 (m) cm^{-1}. UV/Vis ($CHCl_3$): λ (ε, $M^{-1}cm^{-1}$) = 416 (85300), 476 (39300), 567 (94800), 705 (11100), 1045 (19300), 1079 (19700) nm. HR-MALDI-MS (3-HPA): calcd. for $C_{112}H_{106}N_{12}^+$ $[M]^+$ 1618.87; found 1618.87.

Supporting Information (see footnote on the first page of this article): The synthesis and characterization of monoporphyrins **3**–**5**, building block **23**, and precursors **24**–**30**.

Acknowledgments

We thank Dr. Carlo Thilgen for help with the nomenclature and Fabien Choffat for the DSC measurements. This work was supported by the Swiss National Science Foundation (SNF), the National Center of Competence in Research (NCCR) "Nanoscale Science", and the US National Science Foundation (NSF) CHE-0509989.

[1] a) A. Osuka, H. Shimidzu, *Angew. Chem.* **1997**, *109*, 93–94; *Angew. Chem. Int. Ed. Engl.* **1997**, *36*, 135–136; b) A. Nakano, T. Yamazaki, Y. Nishimura, I. Yamazaki, A. Osuka, *Chem. Eur. J.* **2000**, *6*, 3254–3271; c) N. Aratani, A. Osuka, Y. H. Kim, D. H. Jeong, D. Kim, *Angew. Chem.* **2000**, *112*, 1517–1521; *Angew. Chem. Int. Ed.* **2000**, *39*, 1458–1462; d) N. Aratani, A. Osuka, *Chem. Rec.* **2003**, *3*, 225–234; e) D. Kim, A. Osuka, *Acc. Chem. Res.* **2004**, *37*, 735–745; f) S. Hiroto, A. Osuka, *J. Org. Chem.* **2005**, *70*, 4054–4058; g) N. Aratani, A. Takagi, Y. Yanagawa, T. Matsumoto, T. Kawai, Z. S. Yoon, D. Kim, A. Osuka, *Chem. Eur. J.* **2005**, *11*, 3389–3404; h) T. Ikeda, J. M. Lintuluoto, N. Aratani, Z. S. Yoon, D. Kim, A. Osuka, *Eur. J. Org. Chem.* **2006**, 3193–3204.

[2] a) A. Tsuda, A. Osuka, *Science* **2001**, *293*, 79–82; b) A. Tsuda, A. Osuka, *Adv. Mater.* **2002**, *14*, 75–79.

[3] a) Y. H. Kim, D. H. Jeong, D. Kim, S. C. Jeoung, H. S. Cho, S. K. Kim, N. Aratani, A. Osuka, *J. Am. Chem. Soc.* **2001**, *123*,

76–86; b) H. S. Cho, D. H. Jeong, S. Cho, D. Kim, Y. Matsuzaki, K. Tanaka, A. Tsuda, A. Osuka, *J. Am. Chem. Soc.* **2002**, *124*, 14642–14654; c) N. Aratani, A. Osuka, H. S. Cho, D. Kim, *J. Photochem. Photobiol. C* **2002**, *3*, 25–52; d) H. S. Cho, H. Rhee, J. K. Song, C. K. Min, M. Takase, N. Aratani, S. Cho, A. Osuka, T. Joo, D. Kim, *J. Am. Chem. Soc.* **2003**, *125*, 5849–5860; e) D. Kim, A. Osuka, *J. Phys. Chem. A* **2003**, *107*, 8791–8816; f) Y. Nakamura, I.-W. Hwang, N. Aratani, T. K. Ahn, D. M. Ko, A. Tagaki, T. Kawai, T. Matsumoto, D. Kim, A. Osuka, *J. Am. Chem. Soc.* **2005**, *127*, 236–246.

[4] F. Cheng, S. Zhang, A. Adronov, L. Echegoyen, F. Diederich, *Chem. Eur. J.* **2006**, *12*, 6062–6070.

[5] a) D. Bonifazi, F. Diederich, *Chem. Commun.* **2002**, 2178–2179; b) D. Bonifazi, M. Scholl, F. Y. Song, L. Echegoyen, G. Accorsi, N. Armaroli, F. Diederich, *Angew. Chem.* **2003**, *115*, 5116–5120; *Angew. Chem. Int. Ed.* **2003**, *42*, 4966–4970; c) N. Armaroli, G. Accorsi, F. Song, A. Palkar, L. Echegoyen, D. Bonifazi, F. Diederich, *ChemPhysChem* **2005**, *6*, 732–743; d) D. Bonifazi, G. Accorsi, N. Armaroli, F. Song, A. Palkar, L. Echegoyen, M. Scholl, P. Seiler, B. Jaun, F. Diederich, *Helv. Chim. Acta* **2005**, *88*, 1839–1884.

[6] a) T. Ikeue, K. Furakawa, H. Hata, N. Aratani, H. Shinokubo, T. Kato, A. Osuka, *Angew. Chem.* **2005**, *117*, 7059–7061; *Angew. Chem. Int. Ed.* **2005**, *44*, 6899–6901; b) S. Shimizu, A. Osuka, *Eur. J. Inorg. Chem.* **2006**, 1319–1335.

[7] a) J.-Y. Zheng, K. Tahiro, Y. Hirabayashi, K. Kinbara, K. Saigo, T. Aida, S. Sakamoto, K. Yamaguchi, *Angew. Chem.* **2001**, *113*, 1909–1913; *Angew. Chem. Int. Ed.* **2001**, *40*, 1857–1861; b) D. Sun, F. S. Tham, C. A. Reed, L. Chaker, P. D. W. Boyd, *J. Am. Chem. Soc.* **2002**, *124*, 6604–6612; c) P. D. W. Boyd, C. A. Reed, *Acc. Chem. Res.* **2005**, *38*, 235–242.

[8] a) D. Bonifazi, H. Spillmann, A. Kiebele, M. de Wild, P. Seiler, F. Cheng, T. Jung, F. Diederich, *Angew. Chem.* **2004**, *116*, 4863–4867; *Angew. Chem. Int. Ed.* **2004**, *43*, 4759–4763; b) D. Bonifazi, A. Kiebele, M. Stöhr, T. Jung, F. Cheng, F. Diederich, H. Spillmann, *Adv. Funct. Mater.* **2007**, online.

[9] a) A. Giraudeau, H.-J. Callot, J. Jordan, I. Ezhar, M. Gross, *J. Am. Chem. Soc.* **1979**, *101*, 3857–3862; b) A. Giraudeau, L. Ruhlmann, L. El Kahef, M. Gross, *J. Am. Chem. Soc.* **1996**, *118*, 2969–2979.

[10] J. P. Collman, C. S. Bencosme, R. R. Durand Jr, R. P. Kreh, F. C. Anson, *J. Am. Chem. Soc.* **1983**, *105*, 2699–2703; J. A. Cowan, J. K. M. Sanders, *J. Chem. Soc. Chem. Commun.* **1985**, 1213–1214.

[11] F. Li, S. Gentemann, W. A. Kalsbeck, J. Seth, J. S. Lindsey, D. Holten, D. F. Bocian, *J. Mater. Chem.* **1997**, *7*, 1245–1262; P. Hascoat, S. I. Yang, R. K. Lammi, J. Alley, D. F. Bocian, J. S. Lindsey, D. Holten, *Inorg. Chem.* **1999**, *38*, 4849–4853.

[12] a) A. Osuka, K. Maruyama, N. Mataga, T. Asahi, I. Yamazaki, N. Tamai, *J. Am. Chem. Soc.* **1990**, *112*, 4958–4959; b) A. Osuka, F. Kobayashi, K. Maruyama, N. Mataga, T. Asahi, T. Okada, I. Yamazaki, Y. Nishimura, *Chem. Phys. Lett.* **1993**, *201*, 223–228; c) H. S. Cho, D. H. Jeong, M.-C. Yoon, Y. H. Kim, Y.-R. Kim, D. Kim, S. C. Jeoung, S. K. Kim, N. Aratani, H. Shinmori, A. Osuka, *J. Phys. Chem. A* **2001**, *105*, 4200–4210.

[13] D. P. Arnold, G. A. Heath, D. A. James, *J. Porphyrins Phthalocyanines* **1999**, *3*, 5–31.

[14] a) T. Ogawa, Y. Nishimoto, N. Yoshida, N. Ono, A. Osuka, *Angew. Chem.* **1999**, *111*, 140–142; *Angew. Chem. Int. Ed.* **1999**, *38*, 176–179; b) S. Richeter, C. Jeandon, R. Ruppert, H. J. Callot, *Chem. Commun.* **2001**, 91–92; c) S. Richeter, C. Jeandon, J.-P. Gisselbrecht, R. Ruppert, H. J. Callot, *J. Am. Chem. Soc.* **2002**, *124*, 6168–6179.

[15] a) A. Tsuda, A. Nakano, H. Furuta, H. Yamochi, A. Osuka, *Angew. Chem.* **2000**, *112*, 572–575; *Angew. Chem. Int. Ed.* **2000**, *39*, 558–561; b) A. Tsuda, H. Furuta, A. Osuka, *Angew. Chem.* **2000**, *112*, 2649–2652; *Angew. Chem. Int. Ed.* **2000**, *39*, 2549–2552; c) A. Tsuda, H. Furuta, A. Osuka, *J. Am. Chem. Soc.* **2001**, *123*, 10304–10321; d) A. Tsuda, Y. Nakamura, A. Osuka, *Chem. Commun.* **2003**, 1096–1097.

[16] a) P. J. Chmielewski, *Angew. Chem.* **2004**, *116*, 5773–5776; *Angew. Chem. Int. Ed.* **2004**, *43*, 5655–5658; b) H. Segawa, D. Machida, Y. Senshu, J. Nakazaki, K. Hirakawa, F. P. Wu, *Chem. Commun.* **2002**, 3032–3033; c) I. M. Blake, A. Krivokapic, M. Katterle, H. L. Anderson, *Chem. Commun.* **2002**, 1662–1663; d) B. W. Jiang, S.-W. Yang, D. C. Brabini, W. E. Jones Jr, *Chem. Commun.* **1998**, 213–214.

[17] a) J. Wytko, V. Berl, M. McLaughlin, R. R. Tykwinski, M. Schreiber, F. Diederich, C. Boudon, J.-P. Gisselbrecht, M. Gross, *Helv. Chim. Acta* **1998**, *81*, 1964–1977; b) C. Clausen, D. T. Gryko, A. A. Yasseri, J. R. Diers, D. F. Bocian, W. G. Kuhr, J. S. Lindsey, *J. Org. Chem.* **2000**, *65*, 7371–7378; c) J. Seth, V. Palaniappan, R. W. Wagner, T. E. Johnson, J. S. Lindsey, D. F. Bocian, *J. Am. Chem. Soc.* **1996**, *118*, 11194–11207; d) S. I. Yang, J. Seth, T. Balasubramanian, D. Kim, J. S. Lindsey, D. Holten, D. F. Bocian, *J. Am. Chem. Soc.* **1999**, *121*, 4008–4018; e) J.-P. Strachan, S. Gentemann, J. Seth, W. A. Kalsbeck, J. S. Lindsey, D. Holten, D. F. Bocian, *J. Am. Chem. Soc.* **1997**, *119*, 11191–11201.

[18] A. Malik, S. L. Reese, S. Morgan, J. S. Bradshaw, M. L. Lee, *Chromatographia* **1997**, *46*, 79–84.

[19] T. Ogawa, Y. Nishmoto, N. Yoshida, N. Ono, A. Osuka, *Angew. Chem.* **1999**, *111*, 140–142; *Angew. Chem. Int. Ed.* **1999**, *38*, 176–179.

[20] M. Kamo, A. Tsuda, Y. Nakamura, N. Aratani, K. Furukawa, T. Kato, A. Osuka, *Org. Lett.* **2003**, *5*, 2079–2082.

[21] W. J. Youngblood, D. T. Gryko, R. K. Lammi, D. F. Bocian, D. Holten, J. S. Lindsey, *J. Org. Chem.* **2002**, *67*, 2111–2117; M. Speckbacher, L. Yu, J. S. Lindsey, *Inorg. Chem.* **2003**, *42*, 4322–4337.

[22] T. X. Lu, J. R. Reimers, M. J. Crossley, N. S. Hush, *J. Phys. Chem.* **1994**, *98*, 11878–11884.

[23] R. Cosmo, C. Kautz, K. Meerholz, J. Heinze, K. Mullen, *Angew. Chem.* **1989**, *101*, 638–640; *Angew. Chem. Int. Ed. Engl.* **1989**, *28*, 604–607.

[24] A. Osuka, N. Tanabe, S. Nakajima, K. Maruyama, *J. Chem. Soc. Perkin Trans. 2* **1996**, 199–203.

[25] N. Ono, H. Tomita, K. Maruyama, *J. Chem. Soc. Perkin Trans. 1* **1992**, 2453–2456.

[26] a) D. G. Davis in *The Porphyrins* (Ed.: D. Dolphin), Academic Press, New York, **1978**, vol. 5, pp. 127–152; b) R. H. Felton in *The Porphyrins* (Ed.: D. Dolphin), Academic Press, New York, **1978**, vol. 5, pp. 53–126.

[27] a) G. D. Dorough, J. R. Miller, F. M. Huennekens, *J. Am. Chem. Soc.* **1951**, *73*, 4315–4320; b) P. J. Spellane, M. Gouterman, A. Antpas, S. Kim, Y. C. Liu, *Inorg. Chem.* **1980**, *19*, 386–391.

[28] a) M. Kasha, *Radiat. Res.* **1963**, *20*, 55–70; b) M. Kasha, H. R. Rawls, M. A. El-Bayoumi, *Pure Appl. Chem.* **1965**, *11*, 371–392; c) H. L. Anderson, *Chem. Commun.* **1999**, 2323–2330.

[29] a) K. M. Kadish, K. M. Smith, R. Guilard, E. Van Caemelbecke, G. Royal, *The Porphyrin Handbook*, Academic Press, Burlington, **1999**, vol. 8, pp. 1–114; b) K. M. Kadish, E. Van Caemelbecke, *J. Solid State Electrochem.* **2003**, *7*, 254–258; c) K. M. Kadish, K. M. Smith, R. Guilard, *The Porphyrin Handbook*, Academic Press, San Diego, **2000**, vol. 9; d) L. A. Bottomley, K. M. Kadish, *Electrochemical and Spectrochemical Studies of Biological Redox Components* (Ed.: K. M. Kadish), American Chemical Society, Washington DC, **1982**; e) K. M. Kadish, B. Boisselier-Cocolios, B. Simonet, D. Chang, H. Ledon, P. Cocolios, *Inorg. Chem.* **1985**, *24*, 2148–2156; f) J. L. Sessler, M. R. Johnson, S. E. Creager, J. C. Fettinger, J. A. Ibers, *J. Am. Chem. Soc.* **1990**, *112*, 9310–9329; g) A. Giraudeau, L. Ruhlmann, L. EI Kahef, M. Gross, *J. Am. Chem. Soc.* **1996**, *118*, 2969–2979.

[30] R. Chitta, L. M. Rogers, A. Wanklyn, P. A. Karr, P. K. Kahol, M. E. Zandler, F. D′Souza, *Inorg. Chem.* **2004**, *43*, 6969–6978.

[31] Y. Le Mest, M. L′Her, N. H. Hendricks, K. Kim, J. P. Collman, *Inorg. Chem.* **1992**, *31*, 835–847.
[32] a) K. M. Kadish, N. Guo, E. V. Caemelbecke, R. Paolesse, D. Monti, P. Tagliatesta, *J. Porphyrins Phthalocyanines* **1998**, *2*, 439–450; b) D. P. Arnold, G. A. Heath, D. A. James, *J. Porphyrins Phthalocyanines* **1999**, *3*, 5–31; c) Q.-K. Zhuang, F. Scholz, *J. Porphyrins Phthalocyanines* **2000**, *4*, 202–208; d) J. Lisowski, M. Grzeszczuk, L. Latos-Grazynski, *Inorg. Chim. Acta* **1989**, *161*, 153–163; e) R. H. Felton, H. Linschitz, *J. Am. Chem. Soc.* **1966**, *88*, 1113–1116; f) K. M. Kadish, C. Araullo, G. B. Maiya, D. Sazou, J.-M. Brabe, R. Guilard, *Inorg. Chem.* **1989**, *28*, 2528–2533.
[33] a) J. Wojaczynski, L. Latos-Grazynski, P. J. Chmielewski, P. Van Calcar, A. L. Balch, *Inorg. Chem.* **1999**, *38*, 3040–3050; b) S. Wolowiec, L. Latos-Grazynski, *Inorg. Chem.* **1994**, *33*, 3576–3586.

Received: May 31, 2007
Published Online: August 21, 2007

